THE PENNSYLVANIA STATE UNIVERSITY
SCHREYER HONORS COLLEGE

DEPARTMENT OF MECHANICAL AND NUCLEAR ENGINEERING

DESIGN, CONSTRUCTION, AND ANALYSIS OF A PERMANENT MAGNET AXIAL FLUX GENERATOR FOR SPECIFIC SITE CONDITIONS

TYLER CHRISTOFFEL
SPRING 2018

A thesis
submitted in partial fulfillment
of the requirements
for a baccalaureate degree
in Mechanical Engineering
with honors in Mechanical Engineering

Reviewed and approved* by the following:

Richard Auhl
Assistant Research Professor
Thesis Supervisor

Hosam Fathy
Associate Professor of Mechanical Engineering
Thesis Reader

Jacqueline O'Connor
Assistant Professor of Mechanical Engineering
Honors Adviser

* Signatures are on file in the Schreyer Honors College.

ABSTRACT

In a modern energy economy undergoing a shift towards renewable and clean energy sources, it is important that universities maintain the ability to participate in ever-advancing research into these energy sources to keep up with the progress in industry. Here at Penn State, a lot of good work is being done by faculty and students to push the boundaries of our understanding and applicable knowledge about everything from energy production to storage to the most efficient ways to use that energy.

One of these areas of advancement is wind energy. With a growing number of eager students and ambitious companies looking to expand their abilities to harness our unlimited supply of wind, it is crucial for Penn State to be able to use all of the resources at its disposal to participate in this quest for new knowledge. One of those resources is a currently underutilized wind turbine at the edge of campus that would be a willing and helpful subject for testing, if not for a mix of mechanical failures and a mismatch with the site's wind resource.

The purpose of this project is to design and construct a new generator for the turbine that will be more effective at generating useful data at the low wind speeds encountered in this area. In pursuit of this goal, a single stage of the generator design was constructed and tested. The generator type being produced is known as an axial flux permanent magnet generator, and while this kind of generator isn't new, the subject generator model for this project is tailor-made for a specific existing mechanical system.

TABLE OF CONTENTS

ABSTRACT i

TABLE OF CONTENTS ii

LIST OF FIGURES iv

ACKNOWLEDGEMENTS vi

Chapter 1 Literature Review 1

1.1 Introduction to the Permanent Magnet Generator 1
1.2 Modifications to the Axial Flux Generator Design 4
1.3 On-Site Wind Conditions and Tower Parameters 6

Chapter 2 Objectives and Initial Design 8

2.1 Design Objectives 8
2.2 Initial Design 10
2.3 Limiting Design Factors 11
2.4 Producing Computer Models 13

Chapter 3 Construction of a Single Stage 15

3.1 Computer Modeling of the Generator 15
3.2 Determination of Production Agenda 20
3.3 Coil Winding 22
3.4 Fabrication of the Generator Stage 26
3.5 Fabrication of the Testing Stand 31

Chapter 4 Performance Data and Discussion 34

4.1 Changes in Predicted Performance and Discussion 34
4.2 Benchtop Dynamometer Test Performance and Discussion 35

Chapter 5 Future Considerations 42

Appendix A: Generator Design Spreadsheet 45

A.1 Prediction of Number of Turns Per Coil 46
A.2 Wire Information 48
A.3 Power and Voltage Prediction 50
A.4 Maximum Current Check 52
A.5 Coil Design 54

A.6 Coil Size Estimation....58
A.7 Coil Size Check....60
A.8 Moment of Inertia Calculation....62
A.9 Gauss Calculator and Magnet Pricing....66

Appendix B List of Components and Technical Drawings of Fabricated Parts....68

B.1 List of Components....69
B.2 Rotor Spacer Drawing....70
B.3 Testing Stand Base Plate....71
B.4 Vertical Testing Stand Wall....72
B.5 Testing Shaft....73
B.6 Rotor Disk....74
B.7 Stator Support Rod....75
B.8 Rotor Body....76
B.9 Stator Body....77

BIBLIOGRAPHY....78

LIST OF FIGURES

Figure 1: Close up view of a SolidWorks model of the designed generator.....13

Figure 2: Isometric view of the stator with coils, as designed in SolidWorks.....16

Figure 3: Isometric view of a single rotor as designed using SolidWorks.....17

Figure 4: Isometric view of generator stage and testing stand assembly. Hidden components: rotor disks, rotor separator tube. Created with SolidWorks.....19

Figure 5: Exterior side of stabilizing "bookend" wall used for coil winding.....23

Figure 6: Interior side of left bookend, with Teflon sheet and feed hole for lead wire.....23

Figure 7: Test wire winding set-up.....25

Figure 8: Testing stage stator with coils inserted.....27

Figure 9: Testing stand shaft with machined key channel.....29

Figure 10: Aluminum Rotor Body.....30

Figure 11: Completed rotor assembly.....31

Figure 12: Completed generator testing stage assembly.....33

Figure 13: Benchtop dynamometer testing set-up.....36

Figure 14: Overlay of predicted RMS voltage with actual 3-phase RMS voltage data.....37

Figure 15: Benchtop dynamometer test graphs of the neutral-to-pole AC voltage output for 100 RPM.....38

Figure 16: Benchtop dynamometer test graphs of the neutral-to-pole AC voltage output for 150 RPM.....39

Figure 17: Benchtop dynamometer test graphs of the neutral-to-pole AC voltage output for 200 RPM.....39

Figure 18: Diagram of theoretical maximum coil size. Not to scale. Image created on Microsoft Word.....60

ACKNOWLEDGEMENTS

I would like to take a moment to thank all of the people who helped make this project and thesis possible.

Richard Auhl, who acted as my supervisor and mentor throughout this process. Your expertise and confidence in me helped make this sometimes-daunting task both manageable and exciting.

Keith Miska, who helped me learn new machining skills that allowed me to fabricate parts I needed for this project.

Dr. Hosam Fathy, my co-supervisor in the Mechanical Engineering Department who ensured that my project stayed on the right track.

Dr. Jacqueline O'Connor, who served as my Honors Adviser during my thesis and made sure I was on top of things with this project and my academic life as a whole during my time as an undergraduate.

My parents Doug and Lisa Christoffel, and my brothers Cameron and Brandon, for providing all of the love and support an engineering student could ask for.

And last but not least, my second family that is the Atlas benefitting THON special interest organization. Your encouragement and belief in me inspired me day in and day out to work the extra hour to see this project through.

Chapter 1

Literature Review

1.1 Introduction to the Permanent Magnet Generator

A generator, in its most basic sense, is a mechanism that takes some form of energy and converts it into a different form of energy. Typically, the generator converts mechanical energy into electrical energy. This electrical energy can then be stored and attached to a load to provide power for any number of applications [1]. For wind turbines, it is common to use electromagnetic generators to convert energy from the wind into electrical energy, with rotational kinetic energy being the intermediate energy conversion in between.

An electromagnetic generator is a generator that utilizes a rotational energy to vary a magnetic flux through coils of wire. According to Faraday's Law, when a magnetic flux is varied through an area enclosed by a conductive material, that material will develop a current and therefore an electrical potential. This electrical potential is known as an electromotive force, and it can be transmitted through a wire and some subsequent components to provide energy to a load [2], [3]. Typical wind turbine generators are constructed to produce a 3-phase AC power output as opposed to a single-phase AC or DC power output, although it is theoretically possible to construct a generator with any number of phases. This 3-phase AC power must be rectified into one DC input in order to be used to charge a battery bank or to more easily feed into a power grid [4].

For many wind turbines, the electromagnetic generators used are called permanent magnet (PM) generators. A permanent magnet is a component that maintains a magnetic field with no power input. These magnets are often made out of rare earth minerals such as neodymium (NdFeB) or some kind of ferromagnetic material [4]. In most cases, rare earth minerals that act as permanent magnets have stronger magnetic fields per unit of mass or volume than their more common ferromagnetic mineral counterparts. Unfortunately, rare earth minerals are, as the name implies, harder to obtain and significantly more expensive than materials like iron and steel. For this reason, the selection of what magnet to use in PM machines is a balance of cost and magnetic properties.

According to Arand [5], PM machines have historically been made in three different set-ups: Transverse Flux (TFPM), Radial Flux (RFPM), and Axial Flux (AFPM). RFPM generators operate by rotating a rotor with permanent magnets fixed on the surface around the outside or inside of a stator core. RFPM machines tend to consist of one or more rotors and one or more stators, depending on the design [6]. The rotor may be inside the stator, outside of it, or both.

TFPM generators are highly variable and can be made in a broad array of configurations depending on the geometry that a designer desires. The typical geometry of a TFPM is not described here as the difference between designs is significant. The TFPM machine works similarly to the RFPM machine by rotating a rotor with permanent magnets, but instead of a radial flux it creates a transverse flux [8].

Axial Flux generators are considered the easiest design to manufacture, since each stage is made of two rotor plates with permanent magnets and one stator plate with conductive wiring. AFPM generators can be made with multiple stages in series with each other, depending on the

desired output. The axial flux generator is the main focus of this paper and it will be investigated in much greater detail further on in this literature review.

TFPM generators are complex to manufacture and are prone to mechanical failures, in addition to having a high flux leakage. This high flux leakage reduces the amount of power that the generator can output. For these reasons, TFPM generators are not widely used and they will not be discussed further. RFPM generators and AFPM generators have been compared somewhat extensively, with AFPM generators generally proving be better in categories of comparison of interest to the researchers [9], [5]. RFPM machines have a higher power output at very high wind speeds (10 m/s and above), but the lack of efficiency at more common moderate speeds has given the advantage to AFPM generators. Since this thesis centers on the construction of a generator for a turbine located in a region with mostly low to moderate wind speeds (2-8 m/s), AFPM generators are the main focus.

According to a number of sources [10], [2], [4], [5], [9], axial flux generators have come to dominate modern research into wind energy systems for their numerous benefits over other kinds of wind energy conversion generators. Axial flux generators boast a tendency to have very low cogging torque, a high efficiency, high durability (due to a simple design), cost effective construction, and relatively quick and simple construction as compared to similar permanent magnet generators.

Axial flux generators tend to be composed of a small list of basic parts, although designers and researchers have worked extensively to vary aspects of common components to try and achieve certain performance specifications. The generator consists of two main sections: the stator assembly and the rotor assembly.

The stator assembly is comprised of a plate and a series of conductive coils arranged in a circle, with each coil being the same radial distance from the center of the plate as the rest of the coils. The coils also must also maintain an equal angular separation from each other as defined by the circle they form [4]. These coils are usually attached to the stator by setting them in a resin. This resin serves a second purpose of protecting the coils from corrosion. A designer may choose to include ferromagnetic cores in this portion of the assembly that act to guide the magnetic field through the coils, increasing the use of the magnetic field from the magnets. Doing so, however, will dramatically increase the cogging torque.

The second major assembly of the axial flux generator is the rotor assembly. The rotor assembly is composed of two circular plates made of some ferromagnetic material with magnets attached to them in a circle. The magnets are arranged in pairs and are aligned in a N-S → N-S manner, with one of the magnets in a pair directly across from its counterpart on the second disk. The magnets can be covered with a thin layer of resin to protect against corrosion and increase the lifespan of the rotor assembly, although the resin is not a structural component as it is in the stator.

Although the basic set-ups are the same, many researchers have modified components of the AFPM generator in order to see if those modifications would further enhance the performance of AFPMs. This research is considered in the subsequent section.

1.2 Modifications to the Axial Flux Generator Design

Many researchers have focused their efforts on making small changes to the already well-accepted AFPM generator design in order to increase performance in a number of categories.

These categories include, but are not limited to, cogging torque, torque density, power efficiency, total cost, weight and size, and long-term energy efficiency.

Arand and Ardebili [2] investigated a number of methods for reducing cogging torque in for an AFPM generator. Cogging torque is a torque that arises from interactions between the magnets and stator components at rest [12]. This phenomenon can greatly increase the minimum wind speed to initiate rotation, reduce the efficiency at low wind speeds, and generate noise in the generator if it is not carefully mitigated. In order to investigate solutions to this problem, Arand and Ardebili compared a method of segmenting the PMs against a method of skewing magnets with relation to the plane of the rotor disk. The method of skewing magnets had been previously implemented and was found to greatly reduce cogging torque at the expense of power output. Arand and Ardebili found that segmenting the PMs radially in three equal sections and shifting each section angularly by 1.5 degrees with respect to each other achieved the same level of cogging torque reduction (87% reduction) as skewing the magnets by 30 degrees does. The segmentation, however, led to much smaller power losses for the same cogging torque reduction as compared to skewing the magnets.

Alternatively, Minaz and Çelebi [13] investigated power production of a generator that eliminated the stator core and used three rotors with two stators instead of the conventional two rotors and one stator. The elimination of the ferromagnetic cores provides a number of benefits to the system as a whole. For one, the lack of several metal cores in the generator greatly reduces the weight of the generator. The rotor and stator assemblies may also be placed closer together, allowing for the addition of more stages of the assembly for more powerful turbines. Additionally, the elimination of cores effectively eliminates cogging torque and iron losses that hinder performance of generators with cores. While it is true that power output decreases in

general with the elimination of the core, Minaz and Çelebi show that the benefit of being able to start at lower wind speeds and the ability to include multiple stages outweigh the power loss in many applications.

1.3 On-Site Wind Conditions and Tower Parameters

Before a generator can be designed, the initial parameters must be determined. For this thesis, the generator is being built for a specific site on the Penn State campus near Medlar Field. There are already electrical and storage systems in place that must play a role in the design of this generator. A previous graduate student, Brian Wallace, worked on a similar project and has included abundant information about the site in both his Master's thesis and his dissertation [14], [15]. Wallace's work centered around methodology for field performance testing of a wind turbine, and he used the same site for his research as will be used in this paper to set the parameters for the axial flux generator to be built. It is therefore important to understand where these parameters are being gathered from, and how they were gathered.

First, it is important to look at the size limitations of the tower. The generator hub sits atop a 50-foot tower. This tower height was chosen to put it above the wakes of a set of trees that act as obstructions to the normal wind flow. This tower is designed to hold a generator that weighs 155 pounds attached to a two-blade design with a 15-foot blade diameter. The swept area is 175 ft^2. The current mechanical system is designed to passively furl at 27 mph, meaning that this is the wind speed that will result in maximum power output for the generator attached. It furls through a side-furling action, but it may continue producing power after furling.

This system currently sends power through a three phase AC output. The current site has a rectifier to turn this three phase AC output into DC for charging the battery bank. The battery bank can be regulated by the controller at 24 VDC, 36 VDC, and 48 VDC. The controller may dump excess load to a “dump load”. Since these systems are in place, and the generator to be designed will be three phase AC, there is little need to completely overhaul the electric systems.

Perhaps the most important information to be recorded about the site itself is data on the wind resource. The tower is located approximately 1050 feet above sea level. The average wind direction is 290 degrees from due north, and this occurs most commonly during peak wind season from October to March in this area. Average daily wind speeds will vary between 5 and 10 mph throughout the year, or about 2.25 – 4.5 m/s. On many days, the site will not experience sufficient wind to reach the cut-in speed of the current assembly. In addition to a low average wind resource, there are trees of similar height to the tower in surrounding area. In general, wind in this area blows from a direction with no interference by the trees, so they are of less concern than the wind speed itself.

Chapter 2

Objectives and Initial Design

2.1 Design Objectives

The purpose of creating this new axial flux generator is ultimately to increase the utility of the Penn State Research Wind Turbine. This turbine is currently located on the northeast part of Penn State's campus, a few hundred feet from Medlar Field. The turbine was initially constructed for research purposes and has been used intermittently for such uses since 2005. Unfortunately, the wind resource at this location is poor. State College generally does not experience sustained high wind speeds, which means there are few days during the year when wind gusts are strong enough to overcome the current generator's cogging torque. The current generator is a radial flux permanent magnet generator, as described in Chapter 1. Average wind speeds at this location range from 2.5 m/s to 4.5 m/s, but on many days even the strongest gusts will not be sufficient to reach cut-in speed for the current generator, which has been estimated to be just under 4 m/s. Radial flux generators produce power more efficiently at high wind speeds but require a higher wind speed in order to start turning, resulting in fewer days when the turbine was operational. Although wind speeds tend to be sufficient in peak wind season (October-March), the weather during this time of year is often prohibitive for work since the facility is not well-protected from the environment. It would be ideal to have a generator in place that could start up at lower wind speeds, so the range of weather conditions suitable for operation can be

expanded. Increasing the number of possible days of operation means increased opportunities to perform research on the operation of the tower. For this reason, it was decided that the ideal replacement generator/turbine assembly should be capable of achieving a cut-in speed of 2 m/s.

Since the purpose of this generator and its associated mechanical turbine assembly is for research, power output is significant only as far as our ability to track that output under different operating conditions and compare it to operation under nominal operating conditions. For this reason, the replacement generator is not intended to produce the same 3 kW that the current generator produces. This generator is being designed with the purpose of increasing the wind turbines utility as a research subject, not to consistently power any machines, although the computer used to track data points may draw on the turbine for power when operational.

Part of the design process for this generator includes designing it to be mechanically compatible with the mechanical portion of the current generator. The generator and its housing must be weather resistant, be able to effectively translate energy from the blades to the generator, and it must not be detrimental to the operation of the tower due to its physical size. The size and shape of the generator must not be too excessive for the tower to hold and remain stiff as it is raised. The generator housing should also be of similar size to the turbine blade hub so that it is not interrupting air flow and causing a reduction in efficiency.

Similar to the current generator, the new axial flux generator will generate 3-phase AC power. The intention is to keep most of the current electrical systems intact and simply integrate the new generator into the overall electro-mechanical system. The final product should result in a robust turbine that starts up at wind speeds regularly achieved at the current turbine site that can be used to track performance under various artificial and natural conditions. However, this phase of the project examines only the design and construction of a single prototype stage of the

generator. The researchers intend to verify the successes and failures of this prototype based upon electrical property measurements of the unloaded generator stage taken using a benchtop dynamometer.

2.2 Initial Design

The first decision to be made before designing this generator was to establish goals for power output. The current generator is rated at a peak of 3 kW, but since the new generator doesn't have a specific power requirement we had to develop this specification on our own. The higher the output, the larger the generator would have to be. With this in mind, the team decided to start working on understanding how changing different aspects of the generator would impact expected power output and generator size. In order to do this, the team adapted a Microsoft Excel spreadsheet with built in calculations that had been used by the Penn State Wind Energy Club to build a much smaller scale competition turbine. This spreadsheet allowed for the input of a target cut-in speed, coil gauge, number turns for the coils, coil dimensions, number of coils and magnets, as well as the magnetic flux through the coils. This spreadsheet shows the power output of a single stage of an axial generator, but these stages are rather thin and can be stacked to add peak power output. The calculated values of interest from this spreadsheet, after the team made its edits, were current density, expected power output, expected voltage output, coil diameter, air gap, overall moment of inertia per stage, and overall price of coils and magnets. As the researchers iterated on the input values, it became clear that there were a few limiting factors to pay the closest attention to.

2.3 Limiting Design Factors

Before the selecting specific parameters for the generator, limiting variables needed to be determined. After some time working with the physical turbine and analyzing different configurations of the generator, the researchers determined a number of values that would guide the subsequent iterative process. The variables that were determined to be limiting factors of the design are as follows: current density in the wire, desired power output, maximum diameter of the stator, maximum voltage output, and RPM at desired power output.

The first limiting factor is the allowable current density in the copper wires. The higher the desired power, the higher the current density would need to be in the coils to reach it. In general, copper wiring has a maximum allowable current density of 6 $\frac{A}{mm^2}$. Running too much more current will overheat the wire and could potentially lead to an electrical fire. This issue could be solved by increasing the size of the coils, increasing the number of turns, or setting a lower desired power output.

The desired power output was set to be based on utility as a research generator, therefore reducing the number of variable factors impacting the current density in the coils as well as other system parameters. As was mentioned in the previous section, the current generator power is rated at 3 kW at 350 RPM. This peak power output corresponds to a wind speed of about 11 m/s with a tip speed ratio of 9 at this rotational frequency. A greater rotational frequency and the blades will be rotating too fast and efficiency will be lost. Since the turbine blades will remain unchanged for the new generator, it was assumed that the tip speed ratio will remain at about 9 for an RPM of 350. For this reason, the desired power output was set for an RPM of 350.

The size of the coils is another limiting factor. A coil can grow in two dimensions. Layers can be added axially or radially. Expanding the coils axially increases the size of the air gap between the magnets, which reduces the magnetic flux through the coil. A lower magnetic flux translates to a lower voltage in the coils, and subsequently lower power. Expanding the coils radially increases the overall diameter of the stator, since coils need to be spaced further apart with greater coil diameters. In order to narrow down the range of possible coil dimensions, it was ideal to set a maximum stator diameter. This stator diameter would be the determining factor for the maximum diameter of the magnet rotor plates as well, since the magnets themselves are set on a circle that is concentric and identical in diameter to the circle connecting to centers of the coils. The housing for the generator would need to be slightly larger in size. In order to avoid excessive air flow interruption, the maximum stator diameter should not be more than an inch greater in diameter than the turbine blade hub cap. Since the hub cap is 15 inches in diameter, the stator plate was limited to 16 inches in diameter.

Finally, the maximum voltage that could be output by the generator at peak operation had to be determined. This maximum output voltage was determined by the capacity of the battery bank that will be used to load the generator during operation. The batteries can be configured up to an equivalent 48 Volts set up. It is unsafe to charge a battery at a voltage more than slightly higher than the battery's rated voltage, as this may cause overheating or even combustion. The overall generator voltage was therefore limited to 48 Volts.

The following task for was to use these limiting factors as boundaries to determine values for the remaining variables. These values were determined by iterating on initial models until the design had values that worked within all parameters and wasn't prohibitively expensive.

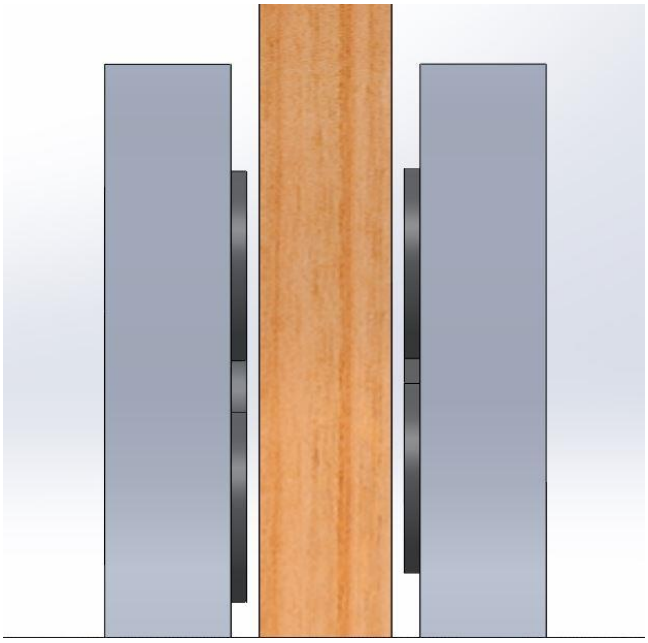

Figure 1: Close up view of a SolidWorks model of the designed generator

2.4 Producing Computer Models

The initial design of the generator was made through an extensive iterative process using a complex Microsoft Excel file. This file was used to outline initial geometrical specifications and to predict power output given user-specified conditions and inputs. Due to the number of variables and the complexity of the interplay between those variables, there was an extensive iterative process using this file in order to make a small number of design prototypes. This sheet is broken down into nine exhibits in Appendix A, with all associated equations given and described.

Initially, the goal was to design for a 3-kW generator with between one and three stages. Stages can be made identically and power outputs can be summed, and since each stage is rather thin it is easy to stack stages of axial flux generators without making the generator excessively extensive along the axis of the generator shaft. The limiting factor in the size of this axial flux

generator was the diameter of the generator, since a diameter much larger than the 15-inch rotor hub currently attached to the Penn State Research Turbine would interrupt air flow while also becoming increasingly difficult to physically mount with size. As a better understanding of the limitations of this generator design was developed, the power output goal was reduced to 1.8 kW. The 3 kW models had resulted in prototype designs that were excessively large in diameter, prohibitively heavy, expensive, or a combination of these three. Since the main intention of this generator is to be usable in a broader range of wind conditions than the current generator, a reduction in power output did not detract from the goals. In fact, a smaller generator would have a smaller moment of inertia, which would be expected to result in a lower cut-in speed.

Ultimately, a decision was made to create three 1.8 kW generator designs: a single-stage generator, a two-stage generator, and a three-stage generator. In general, as the number of stages increases, the amount of power each stage must output is significantly reduced, but the cost of materials and overall weight is increased greatly. The three-stage design was chosen since it was the only model that had a generator diameter as low as 16 inches. This design wouldn't require much more testing than the other models since a single stage could be tested and the performance of a three-stage generator with identical stages could be extrapolated from the performance of the first. This three-stage generator also required less powerful permanent magnets in order to generate the same power output, making it safer to build without being overly expensive.

Chapter 3

Construction of a Single Stage

3.1 Computer Modeling of the Generator

It was decided early on in the design process that a single stage should be tested before multiple were made. Performance data for a single stage would provide good insight for how a generator with multiple identical stages would perform without needing to use labor and material resources for multiple stages. The first stage was tested on a benchtop dynamometer, but before any testing took place a sufficiently sturdy stand had to be made in order to connect the generator to the dynamometer. 8 different designs for parts were created in SolidWorks, but due to required duplicates, a total of 14 components apart from the magnets, coils, bearings, and shaft-dynamometer connector had to be created. The complete parts list can be found in exhibit B.1 of Appendix B. Drawings of all eight components to be fabricated can also be found in Appendix B. The components designed in SolidWorks were as follows: the stator, rotor body, testing stand base plate, rotor disk, generator shaft, testing stand vertical walls, rotor spacer, and the stator support rods. The testing stand base plate was eliminated during production and replaced with a base stand made from two two-by-four planks, but it is included in this section since it was initially a part of the design.

The stator, as discussed in previous sections, holds the coils in place. This component is usually non-metallic, for two reasons. First, if it was a ferromagnetic material it would tend to deflect towards the magnets which could lead to a mechanical failure. Second, since this

generator has to be raised dozens of feet in the air on top of a tower, it is ideal to cut out weight wherever possible. A wooden stator is significantly lighter than a metal one due to the density differences between the materials. The primary concern with wooden stators is that wood tends to fail more quickly than metal in certain environmental conditions. Humidity may cause the stator to warp if it is not properly treated. Alternatively, in dry conditions, the wood will be more likely to ignite if the stator coils reach a high temperature. Since this generator would only be tested inside at low rpms, no additional treatments to the wood were deemed necessary for this phase of testing. Upon the computer modeling stage of the project, it was determined that the coils would be held in the stator by being set in a resin. This decision was later changed and is explained in Section 3.4. The model can be seen in Figure 2.

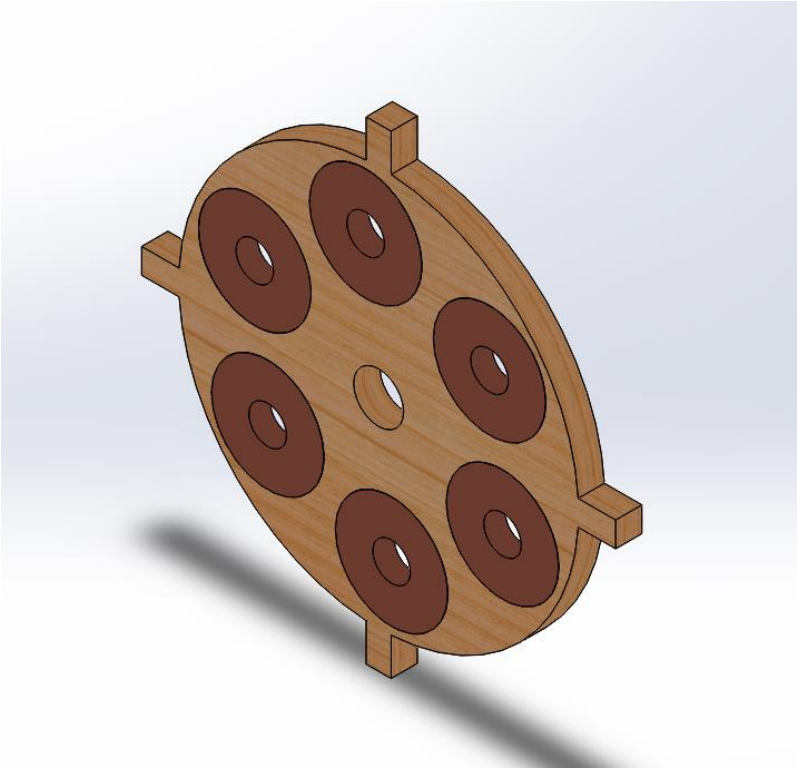

Figure 2: Isometric view of the stator with coils, as designed in SolidWorks

The rotor for this generator was designed in two parts: a rotor body and a rotor disk. The rotor body would be made of aluminum, but the disk would be made of steel. In many generators, the entire rotor plate is made of steel. It is important for a ferromagnetic material to be directly connecting the magnetics within a rotor since this material supports a stronger magnetic field. A rotor made entirely of steel was not feasible since it would be prohibitively heavy and difficult to machine given the equipment available for use in construction. However, a steel disk embedded in an aluminum rotor body would be able to carry the magnetic field without making the rotor disks too heavy or too time-consuming to manufacture. It is probable that this design choice reduced performance of the generator as compared to a rotor made entirely of steel, since there was less medium to carry the magnetic field. In construction of future stages, it would be ideal to find a way to fabricate entirely steel rotors and compare performance. The assembled rotor model can be seen in Figure 3.

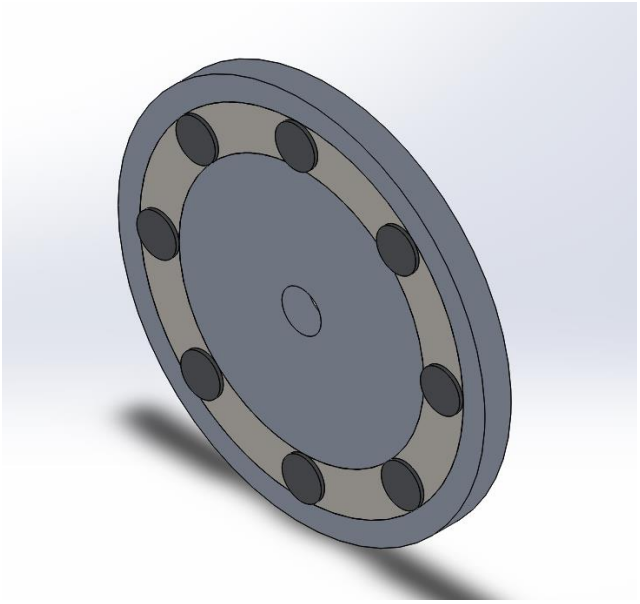

Figure 3: Isometric view of a single rotor as designed using SolidWorks

Although a form of this generator may eventually be used with Penn State's Research Wind Turbine, the stage discussed in this document is meant only for testing. For that reason, a

testing shaft had to be designed to work with the dynamometer. This will likely need to be replaced in later versions. The shaft chosen was 1.5 inches in diameter and made of steel. Steel was selected for it stiffness, and since a number of steel rods of multiple sizes were readily available for use free of cost.

The testing stand base plate was intended to serve to anchor all other components to a track that could move the test subject in and out of contact with the dynamometer. This part was designed to be 1-inch thick and made of plywood. Additional reinforcements of this piece were not included during the computer modelling stage since further support could easily be fabricated during construction if the need arose.

In order to hold the shaft at the proper alignment with the dynamometer, two vertical walls were designed where the shaft bearings could be embedded. In the SolidWorks model, bearings are not included since this part would not be manufactured. These walls were designed to be 1 inch thick and made of plywood in similar fashion to the testing stand base plate.

One of the simplest components in the entire design was the rotor spacer. This component was designed as a precaution to prevent the two rotors from breaking their attachment to the shaft and sliding towards each other due to the strong magnetic force between them. The design tube was 1.05 inches, slightly larger than the designed air gap. This choice was made in the case that the stator ended up thicker than intended, since the tube could always be made thinner. The design material was aluminum, so it would be strong enough to hold the rotors apart but not add a significant amount of weight.

The final designed component in the generator stand assembly was a support rod to run between the vertical walls and suspend the stator. 4 of these would be made, and these rods were

made from standard 3/8”-16 threaded steel rod. These rods were chosen because they were readily available for use.

The overall assembly needed to hold the generator stage at the correct height to attach to the dynamometer, while also supporting the generator stage itself. Since the shaft and rotors were made completely of aluminum and steel, the generator portion of the assembly would be quite heavy for its size. For this reason, some additional support pieces were added to the actual generator stand that aren’t shown in Figure 4.

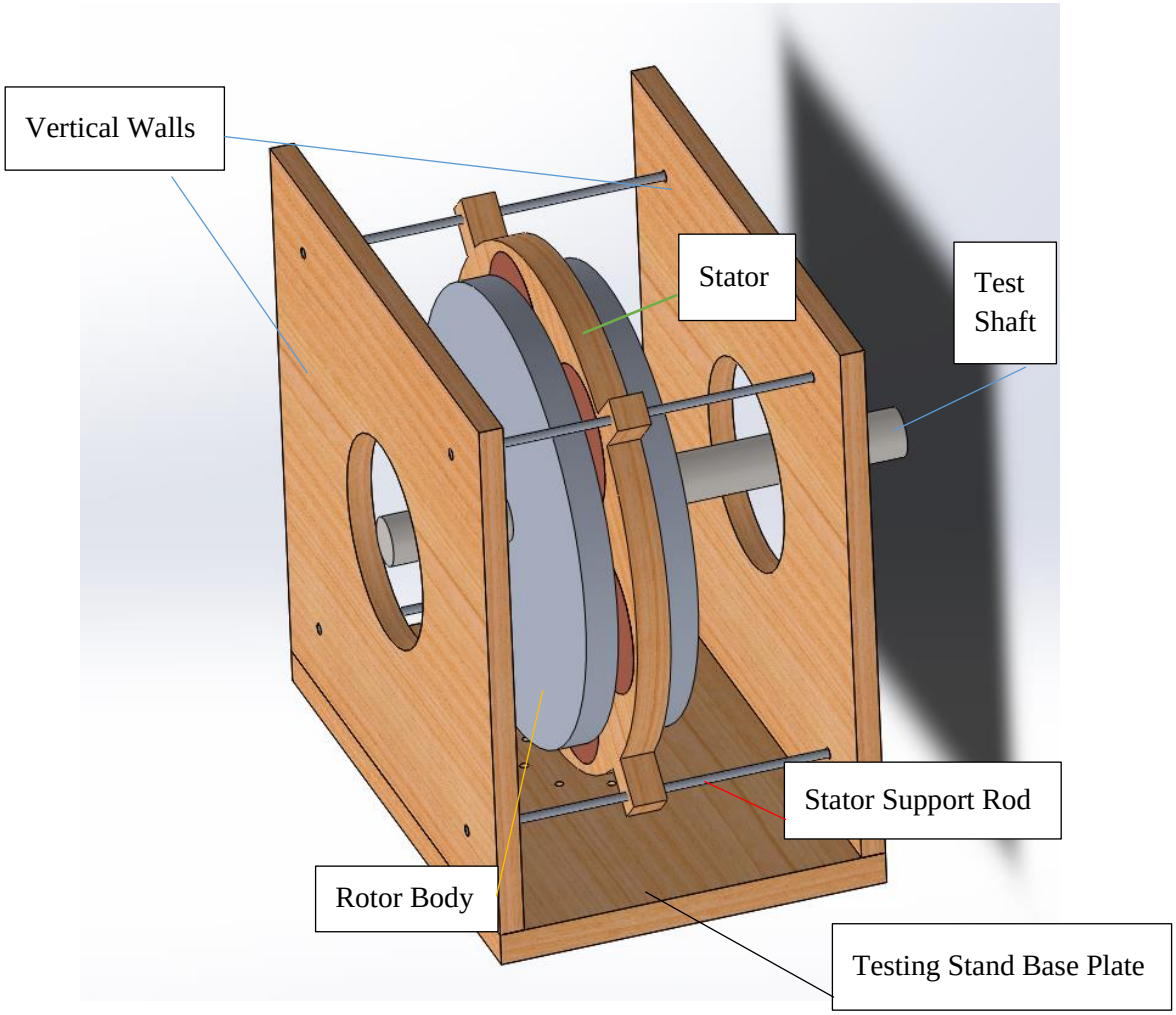

Figure 4: Isometric view of generator stage and testing stand assembly. Hidden components: rotor disks, rotor separator tube. Created with SolidWorks.

3.2 Determination of Production Agenda

Of the many components of the generator that needed to be built by hand, it was determined that there was an ideal order for production of components. It was determined that ideal first step in the construction the generator was the winding of the coils. This decision was made after a number of considerations.

Firstly, one the single most important features of the generator is the total air gap between a pair of magnets. This air gap consists largely of the thickness of the stator, as well as a safety gap on either side as a precaution against rotor plates deflecting enough to contact the stator. Such contact would inevitably lead to mechanical failure of the generator. It is important to keep this air gap as small as possible, since magnetic flux is exponentially related to the gap between the magnets. If the methodology used to create the coils produced coils thicker than predicted, it is possible that magnets of a higher grade would need to be purchased in order to compensate for the loss in magnetic flux by increased air gap size.

The second consideration follows naturally from the first. Permanent magnets are expensive and have proven to be the single largest cost of generator construction. It was therefore fiscally prudent to finish coil winding and measure the electrical and physical properties of these coils before ordering the magnets, in the instance a different set would be required than the magnets initially designed for.

Finally, the design of the rotor and stator were ultimately dependent on the size of the coils. The relation to the stator design is direct since the stators are being made by cutting holes to the size of each coil in a wood board of equal thickness, and then equally spacing the coils in the stator with a single circle connecting the centers. The coil properties are linked to rotor design due to the dependence of the rotor construction on the strength and size of the magnets

used. Smaller-than-intended coils would require stronger magnets, and if the coil circle was reduced in size then the magnet circle would need to be reduced to match it. If either of these are varied from the original design, then the initial rotor design would have to be changed.

The next step in the production process was the creation of the stator. This decision was made based on the relative ease of working with wood versus the steel required for the rotor, as well as the fact that significant differences in the geometry of the stator as compared to its initial design could lead to design changes for the rotor. After the stator, all of the geometry needed to accurately produce the rotors and the generator stand would be available. At this time, with the stator and rotor designs finalized, it was determined that many of the remaining raw materials for required components were already available for use and stored on the ground floor of Hammond. The only components that needed to be purchased were the bearings for the dynamometer mount, the magnets, steel material for the rotor, and an adapter to fit our shaft to the dynamometer. The wood for the stator, resin, steel shaft, rotor spacer, dynamometer, and required fasteners were all available. With materials in order, the only other component initially deemed to be a component that needed to be fabricated was the shaft. The fabrication of components is described in the context of two assemblies: the generator stage and the testing stand. The generator stage includes the testing shaft, the two rotors, the stator, the rotor spacer, the magnets, two bookends to prevent the rotors from sliding, and the coils. Coil winding is described separately due to the significance of this individual process.

Despite best efforts to make the SolidWorks models as close to the intended final product as possible, many of the components had to be altered from their drawings due to material availability, subsequent concept changes, or changes in other parts that a component’s geometry was dependent on.

3.3 Coil Winding

The most time-consuming components of the generator to manufacture were the 6 coils to be inserted into the stator. According to our initial design, the coils were 7 layers deep axially and 17 layers deep radially, meaning a total of 119 turns. They also were supposed to have an inner diameter of 1.5 inches and an outer diameter of about 4.4 inches, with a thickness of 0.57 inches. These values were calculated in Appendix exhibit A.5: Coil Design. The calculations were done by summing the number of layers in a direction multiplied by the thickness of the wire. 0.005 inches per layer were added in anticipation of being unable to wind the coils tight enough to achieve perfect contact between all layers. Even with the built-in tolerance, winding copper coils so tightly without a specialized machine to do so posed a major challenge. A set-up that would make it simple to wind the coils manually while turning a lathe by hand was devised.

The coil-winding set-up on the lathe required 3 components in order to hold the coils in place and confine them to the strict size limits while they were wound. The first component was a 1.5 inch diameter steel shaft that could be inserted into the lathe. The other two components were aluminum discs that were set on either side of the coil and acted as bookends that prevented new turns from sliding off the top of the coil and into a lower layer. These bookends would be used later in conjunction with the rotor spacer to hold the rotor plates in place on the testing shaft. Both bookends had two set screws that made it easy to stabilize the bookends on the shaft during winding, and then to loosen and slide off when it was time to remove the coils. The bookends were 5 inches in diameter so that the outermost radial layers of the coil wouldn’t be at risk of lacking support, since the design coils were 4.4 inches at their outer diameters. A thin Teflon sheet was applied to the surfaces of the bookends that would be in direct contact with the

coil in order to prevent the superglue used to hold layers together from sticking the coils to the bookends. Figures 5 and 6 show the exterior and interior sides of the bookends.

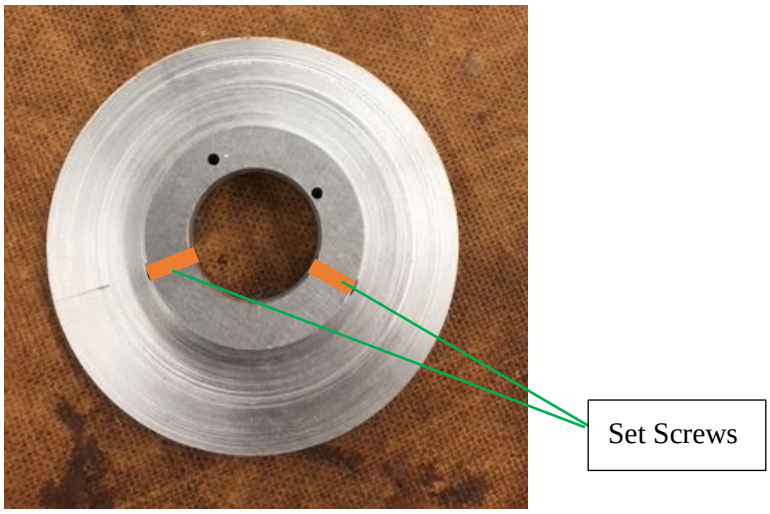

Figure 5: Exterior side of stabilizing "bookend" wall used for coil winding

Figure 6: Interior side of left bookend, with Teflon sheet and feed hole for lead wire

The left bookend had an additional hole drilled through the wall at an angle that would make it close to tangent with the shaft. The purpose of this hole was to allow a lead portion of wire to be fed through and then wrapped around the outside of the coil. This set up ensured the wire wouldn't slide over the shaft as it was rotated. The lead wire would be used later to connect to other coils.

The winding process itself was quite simple. First, the shaft was inserted into the lathe so that about 7 inches of shaft extended past the chucks. The left bookend was then slide onto the shaft until it was about 3 or 4 inches away from the chucks. This separation gave room for the lead portion of wire to loosely wrap around the exposed shaft so it would be out of the way during winding. Following the tightening of the left bookend's screws, WD-40 was applied to the shaft as well as the interior walls of the bookends. The purpose of the WD-40 was to decrease the amount of adhesion between the coil's superglue and the other components of the winding set-up. Subsequently, a portion of wire about 2 feet long was fed through the lead hole and wrapped around the shaft on the outside of the left bookend. As mentioned earlier, this ensured an amount of extra wire existed to form connections while simultaneously anchoring the wire to the bookends and shaft so that it wouldn't slip as it was wound. With everything in place, the first 7 turns of coil were wound in order to create the first layer. Only after this first layer was wound was the right bookend slid onto the shaft. The right bookend could then be pressed against the first layer to achieve a tight layer, after which the bookend was tightened onto the shaft. All following layers were then confined to the same size and would remain tight as they were wound. Superglue was applied by a brush on top of every even layer.

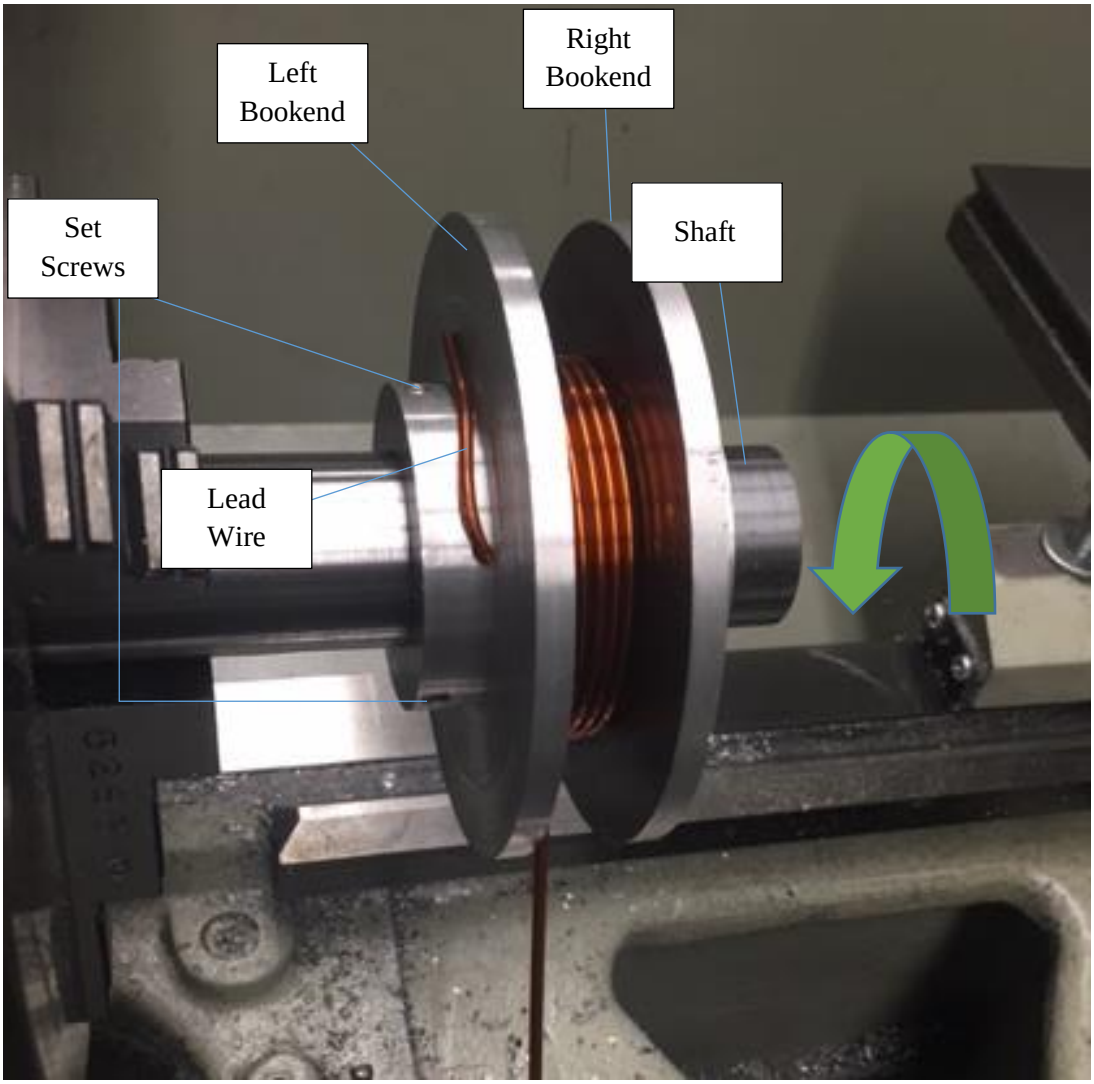

Figure 7: Test wire winding set-up

The test coil shown in Figure 7 above was wrapped without superglue and it expanded forcefully the instant trailing wire was clipped, since its connection to the larger spool of wire held it in tension. The superglue used has a cure time of 2.5 hours, so the coil had to be left in the winding apparatus for at least that amount of time to ensure it wouldn't unwind. Subsequent tests showed that the superglue took closer to 4 hours to fully dry within the coil, most likely due to a low permeability to air of the interior portions of the coil.

One of the largest risks of deviation from original design specifications for the coils was created by the removal of the coils from the winding apparatus. Despite best efforts to reduce adhesion, the coil often became stuck on both the shaft and the bookends. In many cases, the shaft had to be hammered out of the center of the coil. This process had a tendency to detach some of the inner layers from adjacent layers, which would have to be put back in place by hand and in some cases re-glued.

Despite the complications posed by imprecise machinery and a forceful removal process, the coils ended up similar in size to each other. The outer diameter of each coil was approximately 4 inches, although some varied in either direction. This was somewhat significantly smaller than the estimated 4.4-inch outer diameter of the design coils. The coils were also all approximately 0.7 inches thick, although none of them met the intended .57-inch thickness of the design coils. It is possible that more force was applied to hold radial layers together than the axial layers, which would explain a smaller diameter than anticipated but a larger axial thickness. Future efforts to improve winding methods should first determine the exact cause of the discrepancies between the design coils and the manufactured coils, in which case a specific solution could be developed that would produce coils more similar to the design coils than the ones generated through this process.

3.4 Fabrication of the Generator Stage

As mentioned in Section 3.2, the generator stage assembly consists of the stator, rotors, rotor spacer, testing shaft, bookends, coils, and magnets. The fabrication of these components is described in order of completion. The magnets did not need to be altered. The coil manufacturing

process is described in Section 3.3, and these were completed prior to stator construction. The bookends are described in Section 3.3 as well.

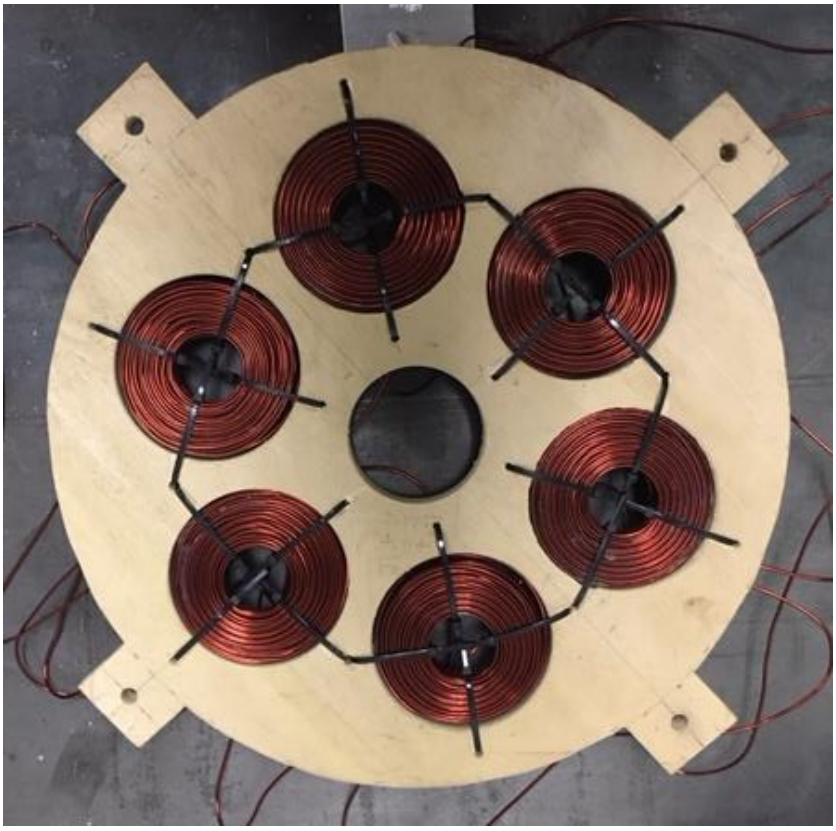

Figure 8: Testing stage stator with coils inserted

The stator designed for testing is likely not the same as the stator to be included in the final generator. The assembled testing stator can be seen in Figure 8. This stator was designed specifically to fit within the testing stand, and if the actual generator design is significantly different it is likely that the new stator would have a different geometry. This testing stator included four rectangular extensions at 90-degree intervals around the outside of the circle that comprises most of the body. These extensions were included so that the four stator support rods could run through the stator without coming in close proximity to the rotor. The original design had each extension being 1 inch thick while overhanging the main body by 1.5 inches. The thickness was increased to 2 inches since a hole would be drilled through the center of each there

would be less risk of the material splitting or otherwise failing with a 2-inch thickness. The center-hole was also expanded from 2 inches to 3 inches to allow for a thicker rotor separator tube to be attached to the rotors, since a thicker separator tube would be better at restricting motion of the rotors. The stator body was designed in SolidWorks to be 1.05 inches thick axially, but the actual production stator was made from ¾ inch plywood. This decision was made so that the stator thickness would match the thickness of the coils as closely as possible. All coils were slightly less than ¾ inches thick, so they all fit within the stator body. The original design planned for coils with a diameter of close to 4.5 inches, but the actual coils ended up being close to 4-inches. Since the coils were all smaller than predicted, it was decided to move the coils closer together in the production stator as compared to the designed stator. This was a significant design change, since it allowed for a plan for smaller rotors. Perhaps the most significant change made to the stator between the model and the production assembly was the method in which the coils were held inside the stator. The original concept had the coils set in resin within the stator, since this is a typical method for holding coils in a stator. It was decided instead to use four zip-ties to hold the coils in place. This decision was made for a number of reasons. First, zip-ties would be easier to work with if mistakes were found in the assembly. Second, the coils would be easily removed from the stator body to be used in future iterations of the generator. Additionally, zip-ties are cheaper and were faster to implement into stator than setting the coils in resin would have been. The drawback of the zip-ties was that they all tended to extend slight past the surface of the coils, causing the air gap to be extended. The final air gap was made to be 1.2 inches in order to accommodate the zip-ties.

The next component created for the generator stage was the testing shaft. This shaft is likely not the same shaft that would be used in the final generator as it is built specifically to be

compatible with the benchtop dynamometer used for testing the generator stage. Although it was designed to be 16 inches long initially, the shaft had to be extended to 20 inches to accommodate the bearings used for the shaft. The shaft and rotors were fabricated to fit with a 3/8-inch by 3/8-inch key. No other changes were made to the shaft from its initial design. The completed testing shaft can be seen in Figure 9.

Figure 9: Testing stand shaft with machined key channel

Following the shaft came the aluminum rotor bodies. A significant design change was made by ordering 1/8-inch magnets that would be stacked in threes, resulting in a magnet thickness of 3/8-inches instead of half an inch as designed. This was due in part to a lack of product availability, but the alternate magnet choice was cheaper while not reducing predicted power output significantly since the new magnets were a much higher grade. This change in magnets resulted in the design for the rotors being changed significantly from the computer model. The production model simplified the aluminum body into a 3/8-inch thick circular plate, without a depression milled into it to hold the rotor disk. Instead, 8 holes were drilled through the plate to house the magnets while the steel rotor disk was attached to the back. This design made the rotor significantly lighter and easier to machine. Although it was intended to be a full inch

thick in the computer model, it was reduced to the thickness of the magnets in production so that when the magnets were inserted into the holes they ended up flush with the surface of the rotor body. Additionally, the diameter of the rotor body was reduced from 14 inches to 12. This change was made due to the fact that the rotor disk holding the magnets could now also be reduced in diameter, given that the coils were moved closer to the center of the stator in the production stator than the designed stator. This reduction in diameter worked to both reduce the weight of the rotors and to decrease the likelihood of detrimental rotor plate deflection due to the pull of the magnets. 8 additional threaded holes were added to attach the rotor disk. The completed aluminum body of one of the two rotors is seen in Figure 10.

Figure 10: Aluminum Rotor Body

The rotor disks were changed somewhat significantly for the final product. The new rotor disk had an outer diameter of 11 inches and an inner diameter of 4.5 inches, as opposed to the designed outer diameter of 12.35 inches and an inner diameter of 9.35 inches. The rotor disk was also moved to the back of the rotor body. These changes were made due to the new design being

easier to accomplish on the available machinery given limited time to finish this part of the generator. Figure 11 shows the completed rotor assembly.

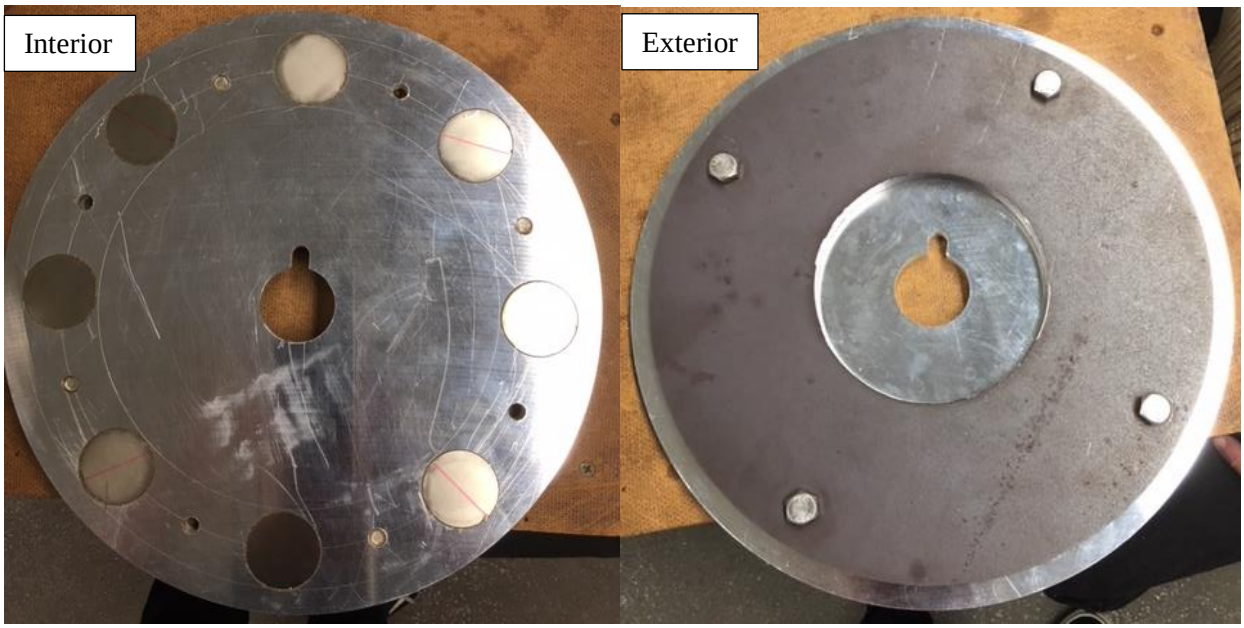

Figure 11: Completed rotor assembly

The final component of the generator stage assembly was the aluminum rotor spacer. The spacer was made to be 1.2 inches thick to match the air gap with the final stator geometry taken into account. It was decided to increase the thickness of the walls of the spacer as compared to the computer model in order to make it more effective at resisting the tendency of the magnetized rotors to attract each other.

3.5 Fabrication of the Testing Stand

The testing stand consists of the two vertical support walls, two base supports, and the four stator support rods. This stand was built to align and support the testing stage of the generator during its performance testing on a benchtop dynamometer.

The vertical walls were made with ¾-inch plywood (actual measurement of 0.69-inches). The holes in the center of each wall were reduced in size to 2 inches, large enough ensure no interference with the shaft while minimizing the loss of structural integrity. The bearings for the shaft were attached on the outside of these walls. No other dimensions had to be altered for these components from the computer models.

The testing stand base plate that was originally designed in the computer model was replaced by two parallel two-by-four wood planks with channels cut out to allow for the vertical walls and the stator to rest in. This setup was preferable as the channel depth could be adjusted to precisely match the height of the generator shaft to the height of the dynamometer shaft.

The stator support rods had to be extended to 14 inches long from the original 8 inches from the computer model. The production rods were made of aluminum and were threaded, making it simple to stabilize them in the apparatus. The threaded supports allowed for these rods to be used to solidly position the stator at any point along the length of the rods, while simultaneously being able to support the vertical walls against buckling. Figure 12 shows a side-view and top-view of the fully assembled testing stage and stand.

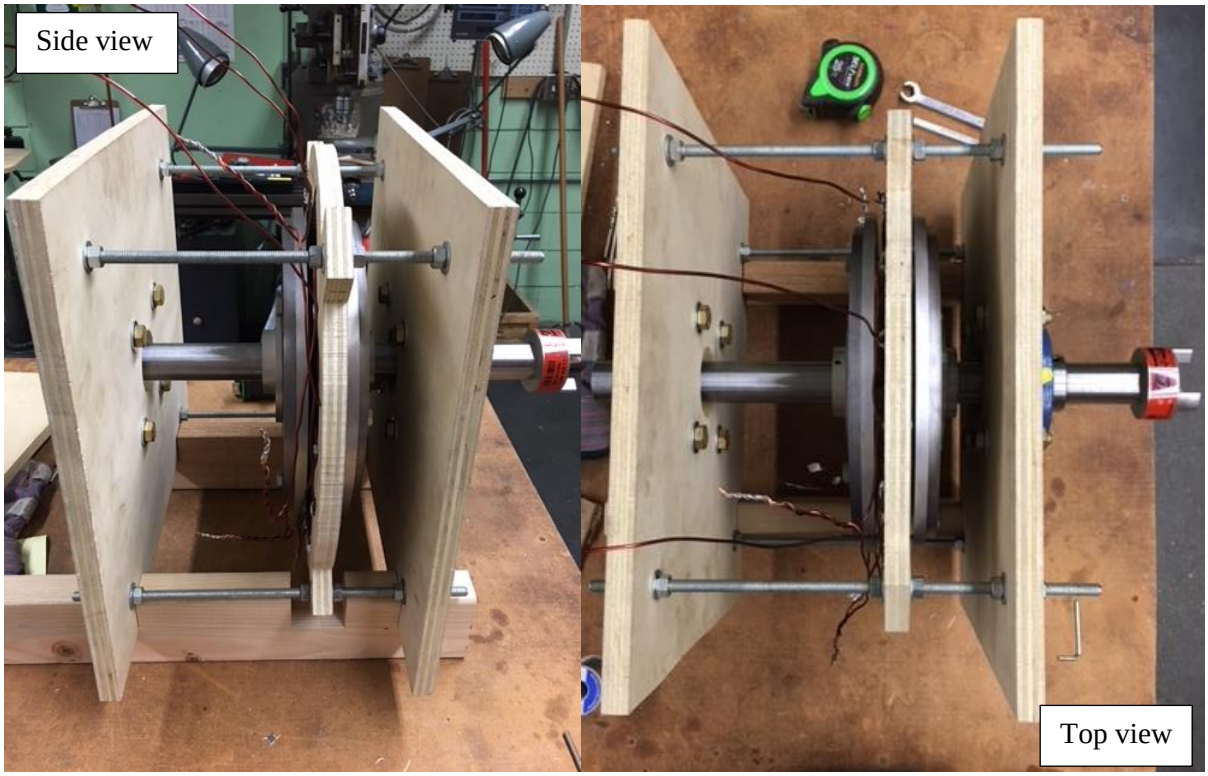

Figure 12: Completed generator testing stage assembly

Chapter 4

Performance Data and Discussion

In order to analyze the success of the design and construction process, an understanding about how the final product compared to its predicted performance, and how that predicted performance compared to the initial model's predicted performance, had to be developed. This chapter explores the change in predicated performance to compare the initial design to the final, and then does the same for the final generator design's actual performance as it relates to its predicted performance. Due to the fact that testing was done on a dynamometer with no load, the physical test could only show voltage and internal resistance characteristics since no power was produced.

4.1 Changes in Predicted Performance and Discussion

With all of the production design changes taken into account, a final prediction of performance was created. According to the final predictions, the generator should have been able to produce 196 Watts at 350 RPM. This value is much lower than the initially designed 600 Watts. This radical reduction in predicted power output is the result of two changes: an increase in the air gap and a change in the magnet design. The design air gap was 0.77 inches, but the final generator had an air gap of 1inch. This change, combined with the exchange of a 1.5 inch by 0.5-inch N42 magnet for a 0.375 inch stack of N52 magnets, led to a reduction in the gauss produced, which directly impacts the current used for predicting power output. These changes also lowered the predicted RMS voltage output at 350 RPM from 15.9 Volts to 10.9 Volts. Resistance was also examined, although it was impossible to say the exact length of wire in each

coil since they all likely varied by a small number of turns to either side of the intended 119 turns due to winding difficulties.

The radical difference between the initial model's performance predictions and those of the final model show a need for alteration of the initial design process in one specific area. Although Chapter 4 mentions two contributing factors to the differences between the initial and final model in the changed magnets and coil geometry, no conclusions are drawn about the magnets. This is because the change in magnet geometry was due to a change in product availability from the time of the initial design, and this does not prove that the process for planning the geometry was erroneous. It is demonstrable, however, that the coil size prediction from the initial model is inaccurate. According to the initial model, the coils should have been 0.57 inches thick at 7 layers thick axially. This was insufficient, and the actual coils showed a gap between layers of about 0.2 inches. This is easily remedied by altering the equation in the design sheet outlined in Cell 5.3 of Appendix A.5 to include a 0.2-inch buffer for each layer added axially.

4.2 Benchtop Dynamometer Test Performance and Discussion

The physical testing of the generator stage occurred using a benchtop dynamometer. The generator was not loaded, so the measured electrical properties did not include power and current. Data was collected for the neutral-to-pole RMS voltage at various rpms between 25 and 400 for all three phases. A computer and DAQ system were used to graph the AC voltage signal for all three phases as well. The benchtop testing set-up can be seen in Figure 13.

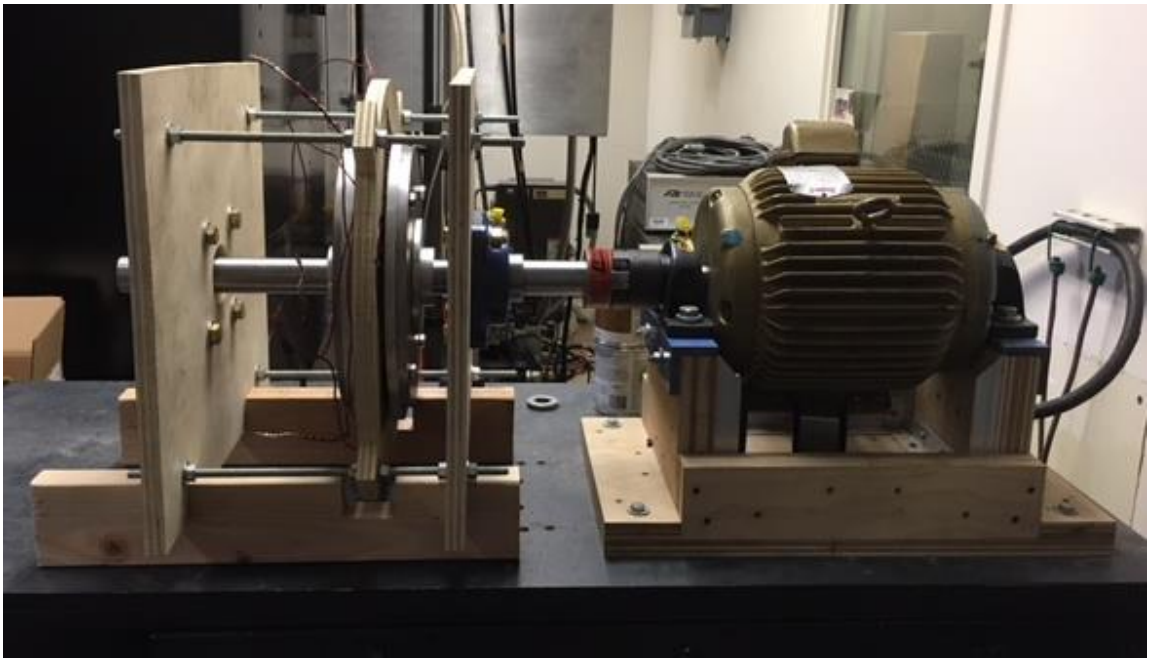

Figure 13: Benchtop dynamometer testing set-up

In order to directly compare the predicted RMS voltage values to those of the actual generator, the outputs of all three phases were tracked using a voltmeter. The measured neutral-to-pole RMS voltage for a single stage of the generator is seen in Figure 14 as the scatter plot, and the predicted RMS voltage is represented as the smooth line on the same graph.

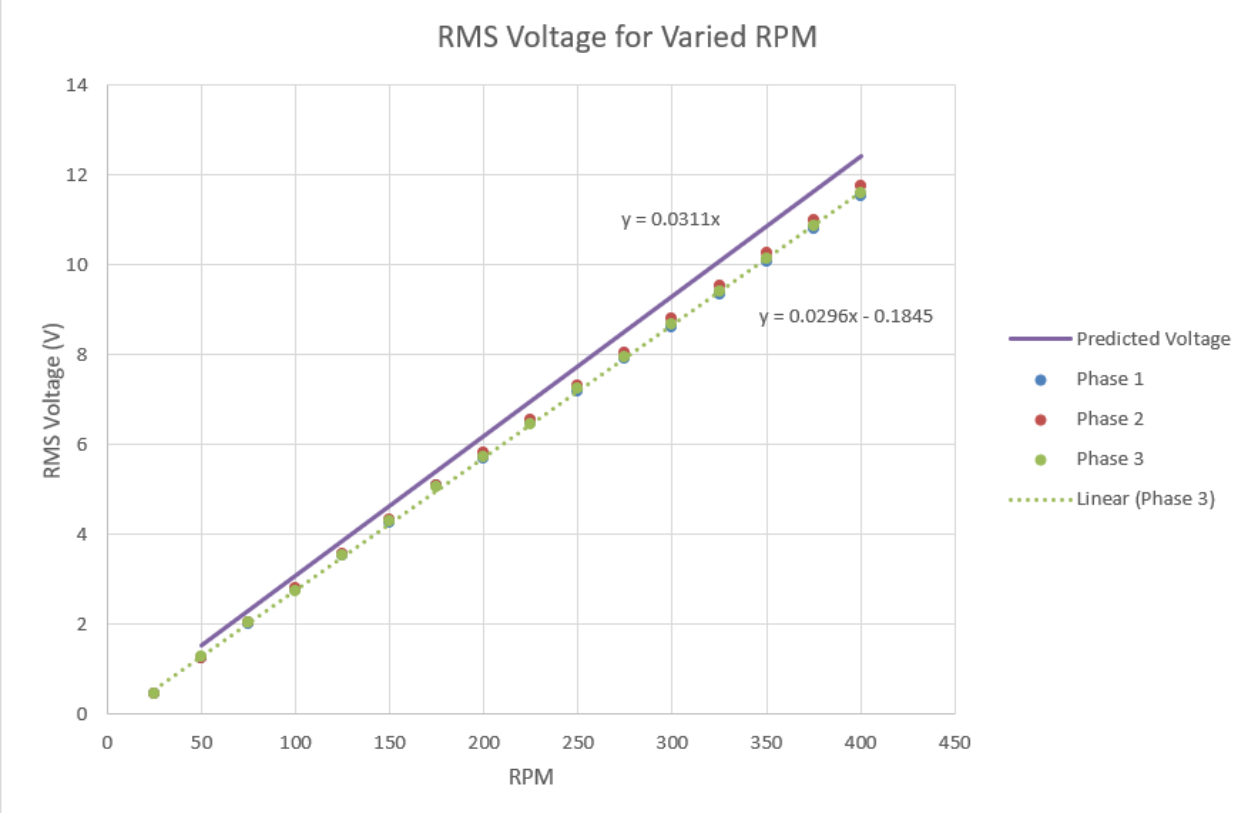

Figure 14: Overlay of predicted RMS voltage with actual 3-phase RMS voltage data

As can be seen in the figure above, all three phases had very similar voltage outputs. The strong similarity between the three phases suggests that the electrical properties of the coils that make up each phase are indeed very similar to each other, although not identical given the small amount of variation. This test validates prediction that RMS voltage should increase linearly with rpm. The slope of the relationship between RMS voltage and RPM is smaller in the real test, although only by 4.8%. At 350 RPM, the voltage is predicted to be 10.88 Volts, while the real test showed an RMS voltage of between 10.08 and 10.27 Volts. It is likely that this slight discrepancy is due to the coils having fewer turns on average than the 119 turns per coil used in the prediction model, although further testing of updated prototype stages would be needed to confidently ascertain the problem. In general, this portion of the testing suggests that the voltage

prediction model is close to accurate for the real-life generator, although it would likely be able to more strongly predict performance of a generator with coils that are exactly as specified in the model.

Apart from validating the design model, the generator was tested to see if it generated voltage in a 3-phase sine wave as predicted for a 3-phase AC generator. This test was performed on the same dynamometer as the one used for the neutral-to-pole RMS voltage testing. A DAQ system was connected to a computer to run the test. The system sampled at 3000 Hz. The voltage was measured neutral-to-pole. This system could not track peak voltage above 10 Volts, so the test was run for 100, 150, and 200 RPM since these RPMs had previously shown values below 10 Volts. Figures 15, 16, and 17 show the data collected for the three tested RPMs, in order of lowest to highest.

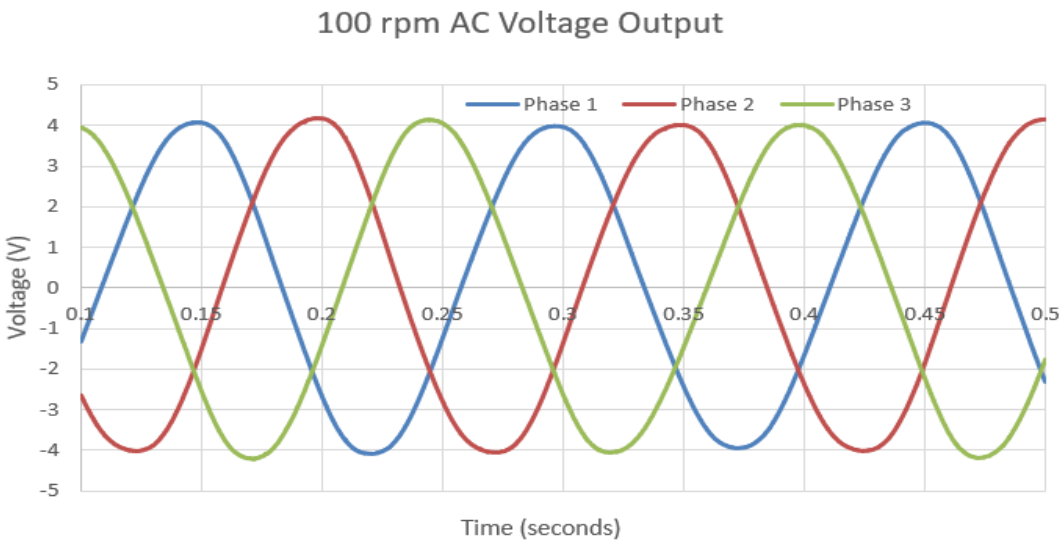

Figure 15: Benchtop dynamometer test graphs of the neutral-to-pole AC voltage output for 100 RPM

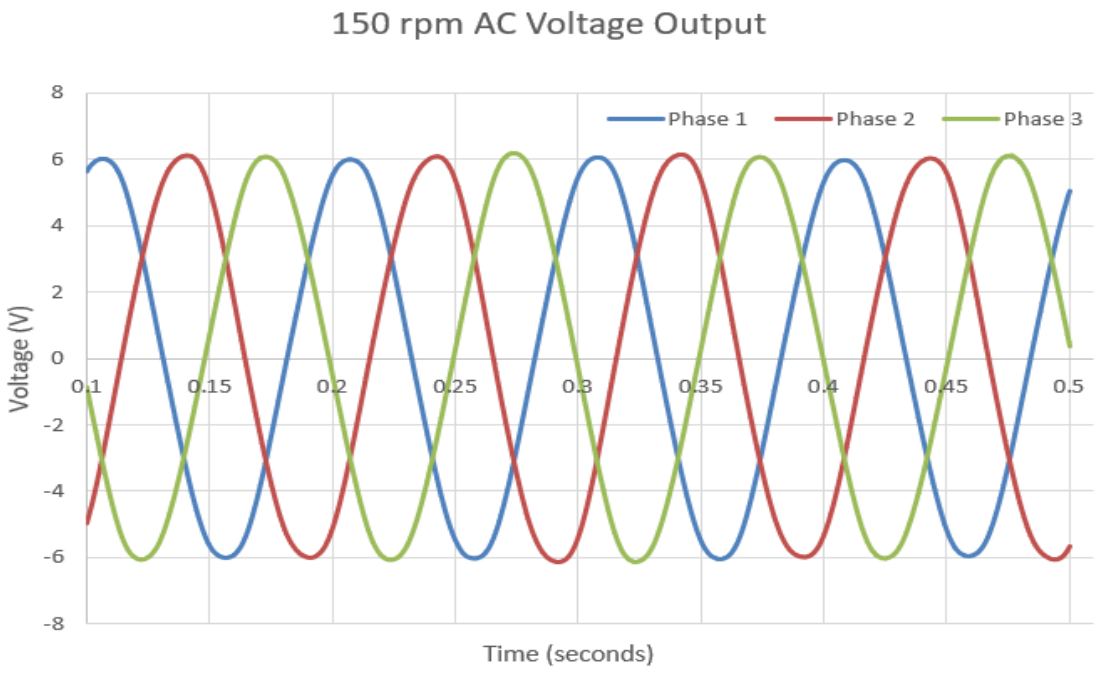

Figure 16: Benchtop dynamometer test graphs of the neutral-to-pole AC voltage output for 150 RPM

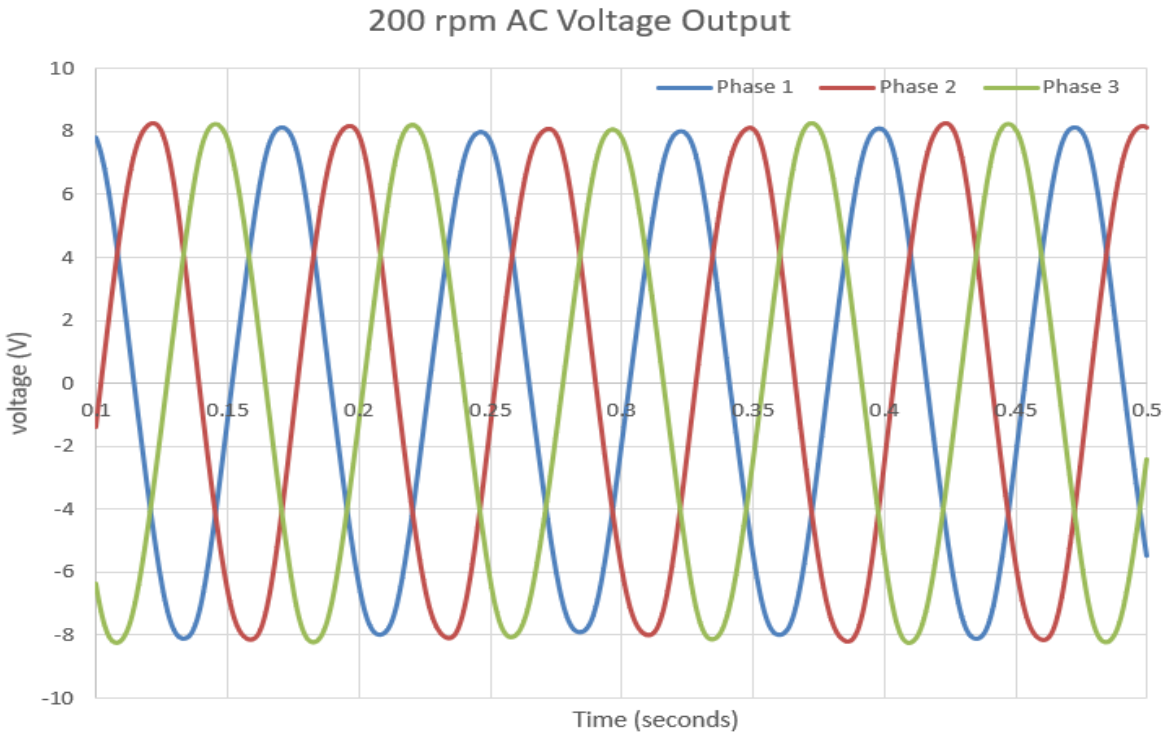

Figure 17: Benchtop dynamometer test graphs of the neutral-to-pole AC voltage output for 200 RPM

In all three RPM tests, the generator produced a clearly sinusoidal voltage output for all three phases. Furthermore, the peak-to-peak voltages for all three phases are similar, although not identical. These results confirm that the physical production of the generator was successful in creating a machine with similar phases that generates voltage in the manner intended. This test confirms what was seen in the RMS voltage test that the phases all vary slightly, since a flat line cannot be drawn across all peaks and troughs. As was mentioned previously, this is likely due to minor variations between the coils used in the stator. It is possible that a mass imbalance on the rotors could have contributed to the unsteady peak-to-peak values, although it was not significant enough to be perceived at the time of testing.

The last portion of design and production validation testing done was a measurement of the resistances of the phases. A measurement of the resistance for each coil from neutral-to-pole and across each phase was attempted. Theoretically, for identical phases, phase-to-phase resistance should be twice that of the neutral to pole resistance.

In the design model, 0.3 Ohms per phase were predicted (neutral-to-pole), meaning phase-to-phase resistance should be twice that at 0.6 Ohms. Both values for the real generator for all three phases and measurements across lines using a typical fluke multimeter were taken. Since these multimeters could not measure resistance with a high resolution, a more sensitive resistance measuring device built into a hot wire anemometer was used to measure resistance as well. The hot wire anemometer device was deemed to be working improperly and the data was disregarded. In addition to the low resolution of the voltmeters, it was found that the cables used to connect the generator outputs to the voltmeters had internal resistances of potentially 0.1 Ohm, although resolution was too low to say for sure. For the neutral-to-pole measurements, all three phases showed a value approximately equal to 0.3 Ohms. While this is the same as the predicted

resistance for one phase, with the internal resistance of the connecting cables considered it is possible the resistance was as low as 0.2 Ohms. The following test measured resistance across two lines for phases 1-2, 2-3, and 3-1. All three tests showed a resistance of between 0.5 and 0.6 Ohms. While it is well within the realm of possibility that these numbers suggest the expected double resistance of phase-to-phase versus neutral-to-pole, the uncertainty is too high to say for sure. Acquisition of more sensitive resistance-measuring equipment is an important part of this project moving forward, but for this portion of testing it was not possible. Ultimately, the resistance measurements were inconclusive and couldn't provide reliable information regarding the resistance properties of the three phases of this generator.

Chapter 5

Future Considerations

At the outset of this project, the intention was to build and test an entire generator in the time allotted as well as mount the generator to the Penn State Research Turbine. As time progressed, it became evident that those goals were quite ambitious and the researchers altered their focus to finishing one stage of a generator model and testing it. During this process, plans continued to be developed for continuations of this project beyond the time allotted for this paper.

The next step in the process is to make revisions to the prototype testing stage generator. It is possible that a redesign of the rotor body to be completely steel would increase the magnetic flux through the stator without having to order stronger magnets. This new rotor would be significantly heavier than the initial testing rotor, and the stand would have to be augmented to support that heavier rotor. Additionally, it is suggested that the coils be removed from the current testing stator and compressed as thin as possible. Thinner coils mean a new stator could be made that is also thinner. This would directly translate into a smaller air gap and increased power output.

With a satisfactorily redesigned single stage, it is simple to create more similar stages. Should the same design be used as was the basis for this project's generator stage, then two more stages should be created to complete the generator. These stages are all mounted on the same

shaft and can be “stacked” quite close to one another, which makes it easy to keep the generator short along its axis. Ideally, all three stages should be tested on the same dynamometer as the prototype single stages were tested on to make the performances directly comparable. This testing apparatus could be similar to the one described in this thesis, albeit with more supports or even different materials for most of the stand since the generator itself will be thrice as heavy.

For these future stages, it is suggested that the coil winding method be updated to create coils with better reproducibility. As was discussed in Chapter 4, difficulties with coil winding is likely one of the biggest contributing factors to the variation in voltage output seen in the benchtop dynamometer testing. Winding by hand made it difficult to smooth out all of the small bends in the wire as it was fed from the stock coil, but a roller mechanism placed between the stock coil and the winding apparatus may adequately straight the wire. This straightened wire would be able to be layered without worry about gaps where wires in adjacent layers could slip into. Apart from hand-winding, the forceful process required to remove the coils from the winding shaft led to variations in coils. This can be solved by eliminating the adhesion of the superglue in the coil to the shaft. A Teflon coating may work for this, although it would slightly extend the diameter of the winding shaft, therefore expanding the inner diameter of the coils. The Teflon used to prevent the bookends from sticking to the coils worked well, so it is a logical addition to the winding shaft to try and prevent the problem of adhesion.

Building the physical generator is only the first part of the problem. This generator is eventually intended to be mounted to the Penn State Research Turbine. Although the entire site was in general disrepair at the beginning of this project, a large amount of time was spent repairing the electrical connections between the tower, the anemometers, and the DAQ systems incorporated into the research site. Before the updated turbine can be used for more research, a

new housing for the generator must be built and then mounted to the tower. In interest of elongating the life of the turbine, every effort should be made to make the housing weather-proof and wear-resistant. It is unlikely the new generator would fit inside the housing for the old since the old generator is a radial flux generator and the two designs are significantly different.

Should the construction of a final, working generator and its subsequent mounting work out well, any further continuation of this project would be the research being done on the operating turbine.

Appendix A: Generator Design Spreadsheet

This appendix describes the utilization and theory behind a Microsoft Excel sheet that was developed to allow designers to input desired parameters and subsequently predict generator performance based on those parameters. The actual spreadsheet is larger than can be wholly inserted into this document. Additionally, understanding the relationship between different exhibits on the spreadsheet from a global scale is difficult without in-depth knowledge of each exhibit at a cell-by-cell level. For these reasons, the spreadsheet has been broken into 9 sections which are first explained individually. Each numerical cell or column is described and designated a cell number of 1.1 – 9.19, with the number preceding the period being the section of the appendix entry (1.X for all cells that appear in section A.1, 2.X for A.2, etc.). Following a description for each cell, the normal iterative process that the designers followed through this spreadsheet is described. A large amount of the equations and theory are taken from [4]. Sections A.7 and A.8 were developed entirely by the designers.

A.1 Prediction of Number of Turns Per Coil

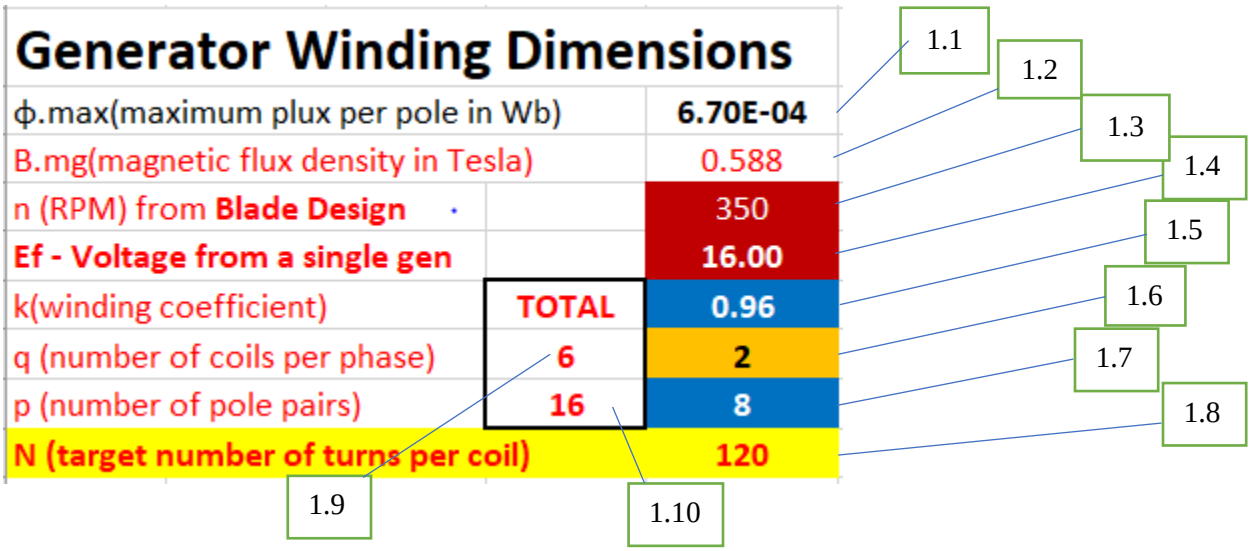

The objective of this section of the spreadsheet is to determine a target number of turns per coil that will be used to guide work through section A.5. First, let's look at each cell.

Cell 1.1 - φ_{max} (maximum flux per pole in Webers [Wb])

- This value is pulled directly from Cell 3.4

Cell 1.2 – Magnetic Flux Density B_{mg} in Tesla [T]

- From Cell 9.5

Cell 1.3 – Estimated rpm of highest generator power output n

- Found to be 350 RPM experimentally, as seen in [14, 15]

Cell 1.4 – Desired voltage output from a single stage of the generator E_f

- Current estimate of 16 Volts based on the maximum capacity of the battery bank, which is rated at 48 volts.

Cell 1.5 – Correction coefficient determined experimentally from previous smaller scale projects k

Cell 1.6 – Number of coils per phase q

- For a 3-phase generator, the total number of coils is 3 times the number of coils for a single phase. This value may be varied to change performance but will drastically alter geometry of stator disk

Cell 1.7 – Number of pole pairs p

- The number of pole pairs should be equal to the total number of coils multiplied by $\frac{4}{3}$

Cell 1.8 – Predicted number of turns per coil N

- Given by the following equation:

$$N = \frac{\sqrt{2} \cdot E_f}{q \cdot 2\pi \cdot k \cdot \varphi_{max} \cdot n \cdot \frac{p}{120}}$$

- Each value is taken from other cells in this exhibit

Cell 1.9 – Total number of coils

- Three times the value of Cell 1.6

Cell 1.10 – Total number of magnets

- Two magnets per pole pair

A.2 Wire Information

Wire Information

2.1 Guage	2.2 Dia. "	2.3 Ohm/Kft
8	0.129	0.6
9	0.114	0.8
10	0.102	1.0
11	0.091	1.3
12	0.081	1.6
13	0.072	2.0
14	0.064	2.5
15	0.0571	3.184
16	0.051	4.0
17	0.045	5.1
18	0.040	6.4
19	0.036	8.1
20	0.032	10.2
21	0.029	12.8

Exhibit A.2 contains useful information of a range of wire gauge options. The black bands define an upper and lower gauge range representing wire gauges with higher potential to work with the designed generator. The wire used to wind the coils must be able to safely carry the predicted current, while also not being too difficult to physically wind into a coil. Wires of a lower gauge (higher diameter) are harder to wind within tight tolerances, while wire of higher gauges (lower diameter) are easier to wind but will not carry as much current. Gauges between 16 and 10 were tested before settling on 12-gauge wire for the generator.

Column 2.1 – Gauge of Wire

Column 2.2 - Diameter of wire corresponding to gauge D_w [in]

Column 2.3 – Resistance Re_w $[\frac{\Omega}{kft}]$ of wire corresponding to gauge

A.3 Power and Voltage Prediction

3.1 3.2 3.3 3.4

1 stage of generators				2 stage of generators			3 stage of generators		
RPM	Volts	Cal I	E Power	Volts	Cal I	E Power	Volts	Cal I	E Power
50	2.27	3.765	8.54	4.54	3.765	17.08	6.81	3.765	25.62
75	3.40	5.648	19.22	6.81	5.648	38.43	10.21	5.648	57.65
100	4.54	7.530	34.16	9.07	7.530	68.33	13.61	7.530	102.49
125	5.67	9.413	53.38	11.34	9.413	106.76	17.01	9.413	160.14
150	6.81	11.295	76.87	13.61	11.295	153.73	20.42	11.295	230.60
175	7.94	13.178	104.62	15.88	13.178	209.25	23.82	13.178	313.87
200	9.07	15.061	136.65	18.15	15.061	273.30	27.22	15.061	409.95
225	10.21	16.943	172.95	20.42	16.943	345.90	30.62	16.943	518.84
250	11.34	18.826	213.52	22.68	18.826	427.03	34.03	18.826	640.55
275	12.48	20.708	258.35	24.95	20.708	516.71	37.43	20.708	775.06
300	13.61	22.591	307.46	27.22	22.591	614.93	40.83	22.591	922.39
325	14.74	24.473	360.84	29.49	24.473	721.68	44.23	24.473	1082.53
350	15.88	26.356	418.49	31.76	26.356	836.98	47.64	26.356	1255.47
375	17.01	28.239	480.41	34.03	28.239	960.82	51.04	28.239	1441.23
400	18.15	30.121	546.60	36.29	30.121	1093.20	54.44	30.121	1639.80

Perhaps the most important exhibit for understand performance expectations, Exhibit A.3 shows voltage, current, and power output predictions for generators of multiple identical stages.

Column 3.1 – RPM of turbine rotors (and subsequently the magnet rotors) n

Column 3.2 – RMS Voltage output E_{pred}

- Given by the following equation

$$E_{pred} = \frac{q \cdot 2\pi \cdot k \cdot \varphi_{max} \cdot n \cdot p \cdot N_{pred}}{120\sqrt{2}}$$

- Variables q, k, φ_{max}, n, and p taken from exhibit A.1. N_{pred} calculated in Cell 5.2

Column 3.3 – Current Prediction I_{pred} [A]

- Given by

$$I_{pred} = \frac{E_{pred}}{2Re_t}$$

- Variable Re_t calculated in Cell 5.6

Column 3.4 – Power Prediction

- Given by $P = I_{pred} \cdot E_{pred}$
- This value is ultimate output parameter of the entire sheet. Given a goal of 1.8 kW overall output, this column was used to check if single stage power output met with the power goals they had set. For a 1-stage generator, this goal was 1.8 kW. For 2 stages, the goal was 900 Watts. For a 3-stage generator, the goal was 600 Watts per stage.

A.4 Maximum Current Check

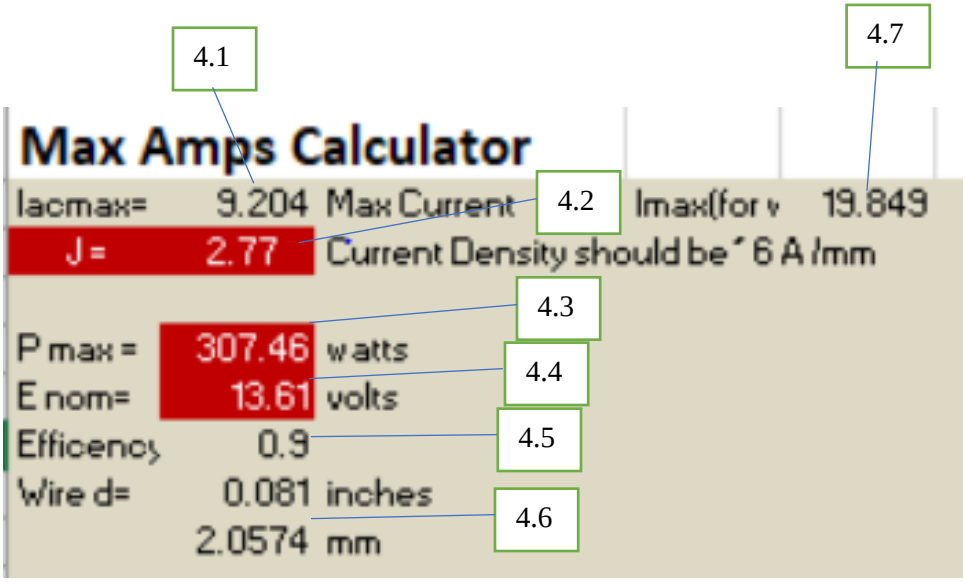

Exhibit A.4 is intended to predict if the given specifications will result in a current density too high for the wire selection to handle. It is most effectively used when performing calculations with voltage and power predictions corresponding to the highest rpm likely to be experienced at the site. See exhibit 3 for predicted values. If Cell 4.2 returns a value greater than 6 for given values, then the design is considered unsafe to use since the wires may overheat.

Cell 4.1 – Predicted maximum AC current I_{acmax} experienced by wires [A]

- Given by

$$I_{acmax} = \frac{1.1 \cdot P}{3 \cdot E_{pred} \cdot \eta}$$

- Values P and E_{pred} are taken from exhibit A.3. These values are chosen from their columns based on which rpm the maximum current needed to be calculated for. In this case, power and predicted voltage values corresponding to 300 rpm were used.
- Generator efficiency η from Cell 4.5

Cell 4.2 – Current Density J $[\frac{A}{mm^2}]$

- Given by

$$J = \frac{I_{acmax}}{A_w}$$

- A_w Calculated using wire diameter in Cell 4.6

Cell 4.3 – Power P

- From Column 3.4

Cell 4.4 – Predicted Voltage E_{pred}

- From Column 3.2

Cell 4.5 – Efficiency of generator η

- Predicted given previous experience

Cell 4.6 – Wire diameter D_w in inches and mm

- From column 2.2

Cell 4.7 – Max tolerable current I_{max} [A]

- Given by

$$I_{max} = 6 \cdot A_w$$

A.5 Coil Design

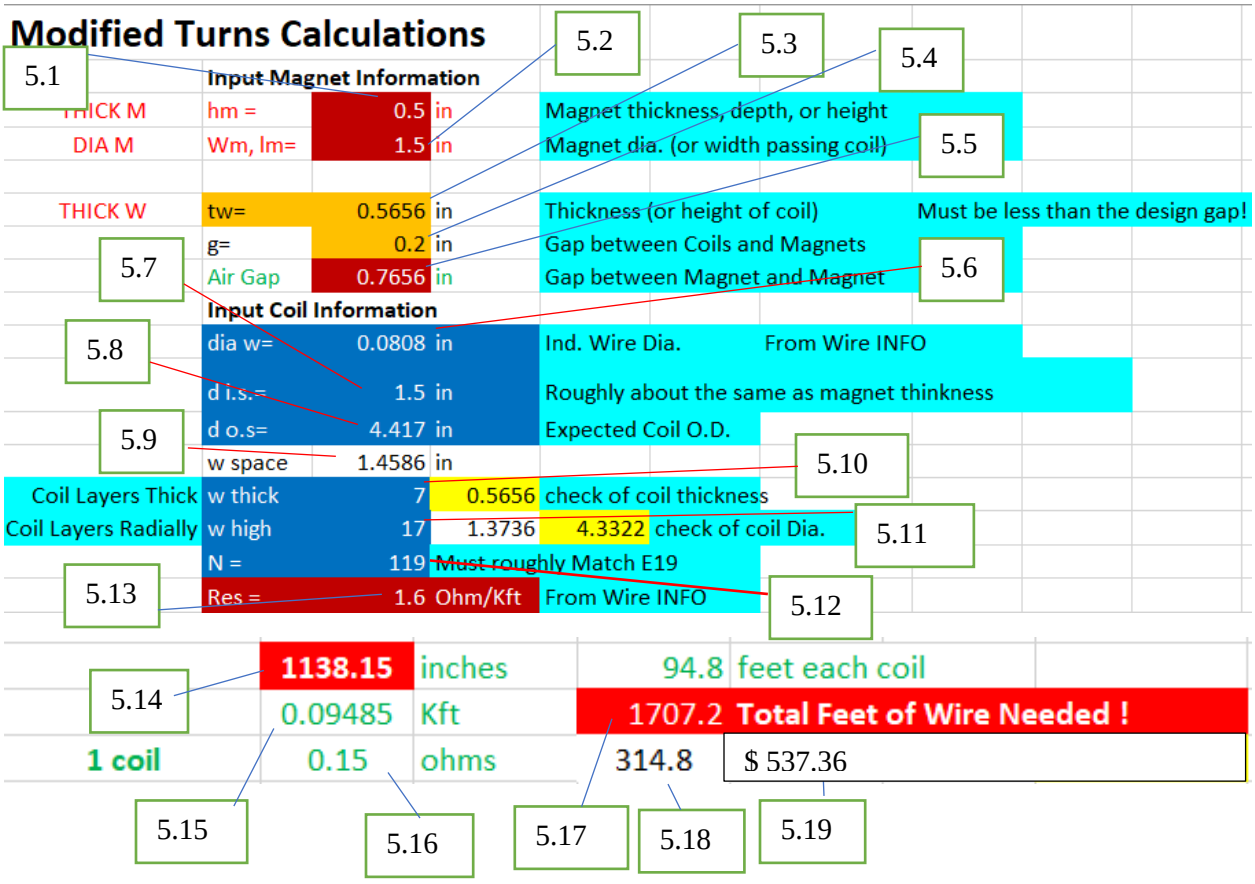

Exhibit A.5 is used to calculate coil geometry, cost of wire, and the estimated air gap between the magnets. A large focus during the design process was minimizing the predicted air gap while not excessively extending coil diameter. The larger the coil diameter, the larger the stator would need to be to accommodate the coils.

Cell 5.1 – Magnet Thickness t_{mg} [in]

- From Cell 9.3

Cell 5.2 – Magnet Diameter/Width (depending on shape of magnet) W_{mg} [in]

- From Cell 9.2

Cell 5.3 – Axial Thickness of coil t_c [in]

- Calculated as the number of axial layers of wire multiplied by wire diameter. In the sheet, this is calculated as Cell 5.6 multiplied by Cell 5.10. Imprecise winding was not factored into this calculation.

Cell 5.4 – Planned additional air gap G [in]

- This portion of the total air gap is designed into the system in case the rotors begin to deflect towards each other. A larger gap means a lower likelihood of mechanical failure from interference of the stator and rotors but would also mean a lower magnetic flux. A lower magnetic flux would lead directly to a smaller voltage produced and a diminished power output.
- The given value in this exhibit of 0.2 inches means that half of that gap was designed on either side of the stator. With this planned air gap, there should be a gap of 0.1 inch between the stator and the magnets on the rotor directly facing it.

Cell 5.5 – Total Air Gap AG [in]

- Planned air gap G added to the stator thickness t_c
- This gap represents the distance between magnet faces in a pole pair. This gap is used in calculating the magnetic flux through the stator.

Cell 5.6 – Wire Diameter D_w [in]

- From selected gauge in Exhibit A.2

Cell 5.7 – Inner Coil Diameter D_{in} [in]

- Parameter determined by the researchers. It is suggested in [4] that the ideal inner coil space is the same shape as the face of the magnets. In this case, the magnets that were

planned for were 1.5 inches in diameter so the inner coil diameter was set at the same value.

Cell 5.8 – Outer Coil Diameter D_{out} [in]

- Given by

$$D_{out} = D_{in} + 2[L_{rad}(D_w + 0.005)]$$

- L_{rad} found in cell 5.11
- The additional 0.005 inches in the equation was included to account for imprecise winding.

Cell 5.9 – Thickness of the coil band t_{band} [in]

- Given by

$$t_{band} = \frac{D_{out} - D_{in}}{2}$$

Cell 5.10 – Number of axial layers of wire L_{ax}

Cell 5.11 – Number of radial layers of wire L_{rad}

Cell 5.12 – Total number of turns for estimation N_{pred}

- Given by

$$N_{pred} = L_{rad} \cdot L_{ax}$$

- N_{pred} should be similar to value N in Cell 1.8 in order to get similar performance predictions to the input performance goals from exhibit A.1.
- The number of axial layers and radial layers were altered to design a coil that met the requirement for number of turns while not making the coil too large in the radial and axial directions to meet performance goals.

Cell 5.13 – Wire resistance Re_w $[\frac{\Omega}{kft}]$

- Given in Column 2.3

Cell 5.14 – Total length of wire in a single coil l_c [in]

- Taken from last cell in Column 6.3

Cell 5.15 – Conversion of length of wire from inches to kft for l_c

Cell 5.16 – Resistance per coil Re_t [Ω]

- Cell 5.15 multiplied by Re_w

Cell 5.17 – Total length of wire in generator [ft]

- This calculation varies based on the number of stages in the model generator
- Given by

$$l_{tot} = l_c \cdot q \cdot Number\ of\ Stages$$

  - Variable q is the number of coils per stage

Cell 5.18 – Cost of wire per kilofoot of Essex 12 Gauge Magnet Wire, found on Amazon

Cell 5.19 – Total cost of coils in model generator

A.6 Coil Size Estimation

6.1	6.2	6.3	6.4
layer	Dia c w	Circ	Turns
1	1.672	5.25	7
2	1.843	5.79	7
3	2.015	6.33	7
4	2.186	6.87	7
5	2.358	7.41	7
6	2.530	7.95	7
7	2.701	8.49	7
8	2.873	9.03	7
9	3.044	9.56	7
10	3.216	10.10	7
11	3.388	10.64	7
12	3.559	11.18	7
13	3.731	11.72	7
14	3.902	12.26	7
15	4.074	12.80	7
16	4.246	13.34	7
17	4.417	13.88	7
		1138.15	119

Column 6.1 – Radial layer

Column 6.2 – Diameter of coil at corresponding layer

Column 6.3 – Length of wire in coil at radial layer $C_{lay,i}$, with the last cell being the total length of wire needed l_c. Column can be summarized with the following equations.

- Given by

$$l_c = L_{ax} \cdot \sum_{i=1}^{L_{rad}} C_{lay,i}$$

- $C_{lay,i}$ is the circumference of the circle formed by a radial layer [in]

- Given by

$$C_{lay,i} = C_{lay,i-1} + 2\pi(D_w + 0.005)$$

- $C_{lay,1}$ used the circumference of the inner diameter of the coil πD_{in} instead of $C_{lay,i-1}$

Column 6.4 – Number of axial layers per radial layer

A.7 Coil Size Check

Max Coil D Calc	
Stator Radius	8
Number of Co	6
Radial size of	1.0471976
Proposed coil	2.2086
Tolerance Reg	0.125
Distance from	7.875
Maximum all	2.625
Works?	1

7.1
7.2
7.3
7.4
7.5
7.6
7.7
7.8

The purpose of Exhibit A.7 is to check that the designed coils will fit inside the intended stator. If the geometry doesn't work, then the coils must be reduced in diameter, the stator must be expanded, or a balance of both. All equations were derived by the researchers.

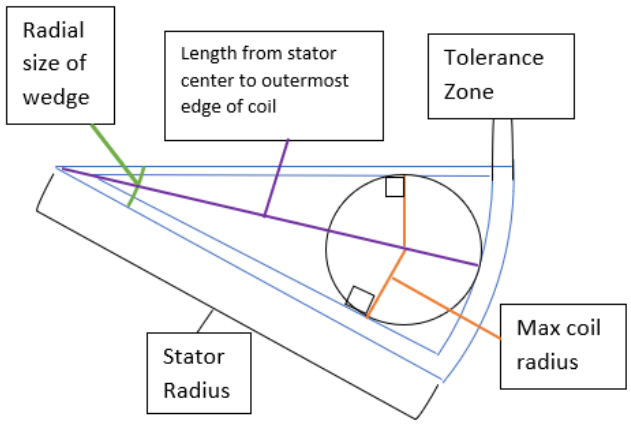

Figure 18: Diagram of theoretical maximum coil size. Not to scale. Image created on Microsoft Word.

Cell 7.1 – Stator radius r_{st} [in]

- A stator radius is entered to be studied. This is one of the main variables under investigation in this exhibit.

Cell 7.2 – Number of Coils q

- From Cell 1.9

Cell 7.3 – Radial size of one wedge of the Stator S [rad]

- Given by

$$S = \frac{2\pi}{q}$$

Cell 7.4 – Proposed Coil Radius r_c [in]

- Half of the outer diameter of the coil, D_{out}

Cell 7.5 – Tolerance Region of wedge t_{wedge} [in]

- Design decision. In this model, the tolerance region is set at 0.125 inches. This region is a band of the set thickness that runs around the perimeter of the wedge that each coil fits into. This region is to ensure adjacent coils are not touching and the coils are not too close to the edge of the stator. Some materials, like the wood intended for use in the stator, have tendencies to split when being machined near thin portions of material. An adequate tolerance region protects against these kinds of failures.

Cell 7.6 – Distance from Stator Center to outermost edge of coil $l_{o\to c}$ [in]

- Given by

$$l_{o\to c} = r_{st} - t_{wedge}$$

Cell 7.7 – Maximum Allowable radius r_{max} [in]

- Given by

$$r_{st} = \frac{l_{o\to c}}{3}$$

Cell 7.8 – IF test. Returns value “1” if the proposed coil radius is less than the maximum allowable radius, “0” if it does not.

A.8 Moment of Inertia Calculation

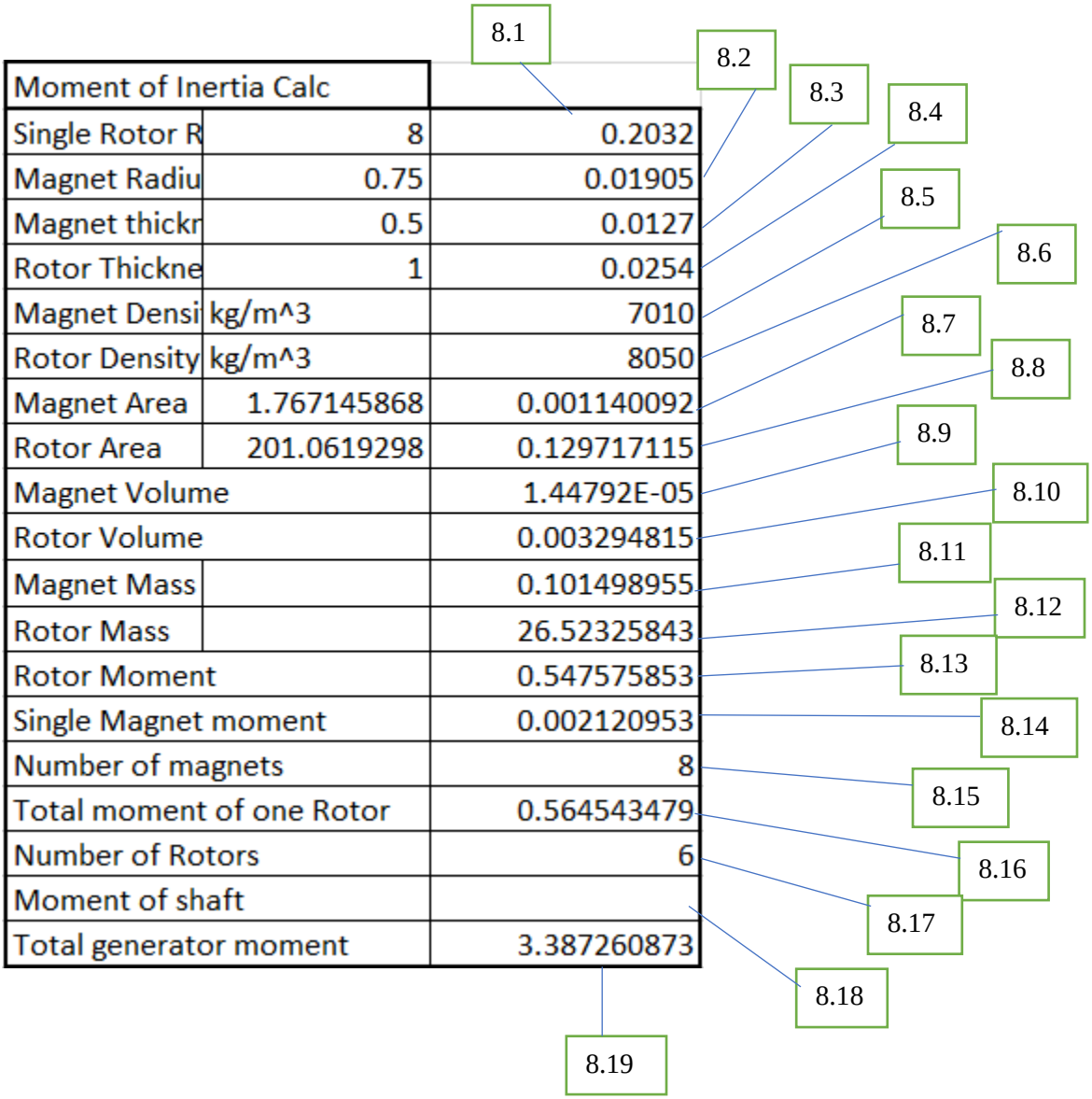

Moment of Inertia Calc		
Single Rotor R	8	0.2032
Magnet Radiu	0.75	0.01905
Magnet thickr	0.5	0.0127
Rotor Thickne	1	0.0254
Magnet Densi	kg/m^3	7010
Rotor Density	kg/m^3	8050
Magnet Area	1.767145868	0.001140092
Rotor Area	201.0619298	0.129717115
Magnet Volume		1.44792E-05
Rotor Volume		0.003294815
Magnet Mass		0.101498955
Rotor Mass		26.52325843
Rotor Moment		0.547575853
Single Magnet moment		0.002120953
Number of magnets		8
Total moment of one Rotor		0.564543479
Number of Rotors		6
Moment of shaft		
Total generator moment		3.387260873

Exhibit A.8 uses estimated information about a number of generator components to estimate the moment of inertia of the generator. This information was not used further but it is useful for future continuations of this project since the moment of inertia will help future

researchers predict the start-up speed of the turbine. All moment calculations were done assuming all objects are cylindrical. Different geometry would require a new table.

Cell 8.1 – Single rotor radius r_{ro} [m]

- Generally taken to be the same as the stator radius, however, the production rotors for the physical generator developed have a smaller radius than the stator in the interest of reducing weight.

Cell 8.2 – Magnet radius r_{mg} [m]

- Half of the magnet diameter from Cell 9.2

Cell 8.3 – Magnet thickness t_{mg} [m]

- From Cell 9.1

Cell 8.4 – Rotor thickness t_{ro} [m]

- Design choice. A thicker rotor will carry more magnetic field and would be stiffer. A rotor thickness of at least the magnet thickness is recommended by [4].

Cell 8.5 – Magnet density ρ_{mg} $[\frac{kg}{m^3}]$

- Density of neodymium magnets found on website of Allstar Magnetics [16].

Cell 8.6 – Rotor density ρ_{ro} $[\frac{kg}{m^3}]$

- Density of steel found on Thyssenkrupp Aerospace website [17]

Cell 8.7 – Magnet area A_{mg} $[m^2]$

- Given by

$$\pi \cdot r_{mg}{}^2$$

Cell 8.8 – Rotor area A_{ro} $[m^2]$

- Given by

$$\pi \cdot r_{ro}{}^{2}$$

Cell 8.9 – Magnet Volume V_{mg} $[m^3]$

- Given by

$$V_{mg} = A_{mg} \cdot t_{mg}$$

Cell 8.10 – Rotor volume V_{ro} $[m^3]$

- Given by

$$V_{ro} = A_{ro} \cdot t_{ro}$$

Cell 8.11 – Magnet mass m_{mg} [kg]

- Given by

$$m_{mg} = \rho_{mg} \cdot V_{mg}$$

Cell 8.12 – Rotor mass m_{ro} [kg]

- Given by

$$m_{ro} = \rho_{ro} \cdot V_{ro}$$

Cell 8.13 – Rotor moment M_{ro} $[kg \cdot m^2]$

- Given by

$$M_{ro} = 0.5 \cdot m_{ro} \cdot r_{ro}{}^{2}$$

Cell 8.14 – Single magnet moment about the central axis M_{mg} $[kg \cdot m^2]$

- Given by

$$M_{mg} = \left(0.5 \cdot m_{mg} \cdot r_{mg}{}^{2}\right) + \left(m_{mg} \cdot \left[\, r_{st} - t_{wedge} - t_{band} - \frac{D_{in}}{2}\right]^2\right)$$

- Variables r_{st} and t_{wedge} from exhibit A.7
- Variables t_{band} and D_{in} from exhibit A.5

Cell 8.15 – Number of magnets on each rotor F_{mg}

- Equal to the number of pole pairs p from Cell 1.7

Cell 8.16 – Moment of a single assembled rotor (magnet and rotor plate) $M_{ro,t}$ $[kg \cdot m^2]$

- Given by

$$M_{ro,t} = M_{ro} + (F_{mg} \cdot M_{mg})$$

Cell 8.17 – Number of rotors F_{ro}

- There are two rotors per stage, so this will depend on the number of stages in the generator model

Cell 8.18 – Moment of shaft M_{shaft}

- This cell was not filled in since no work has been done on planning a shaft for the final generator

Cell 8.19 – Total moment M_{gen}

- Given by

$$M_{gen} = M_{shaft} + (F_{ro} \cdot M_{ro,t})$$

A.9 Gauss Calculator and Magnet Pricing

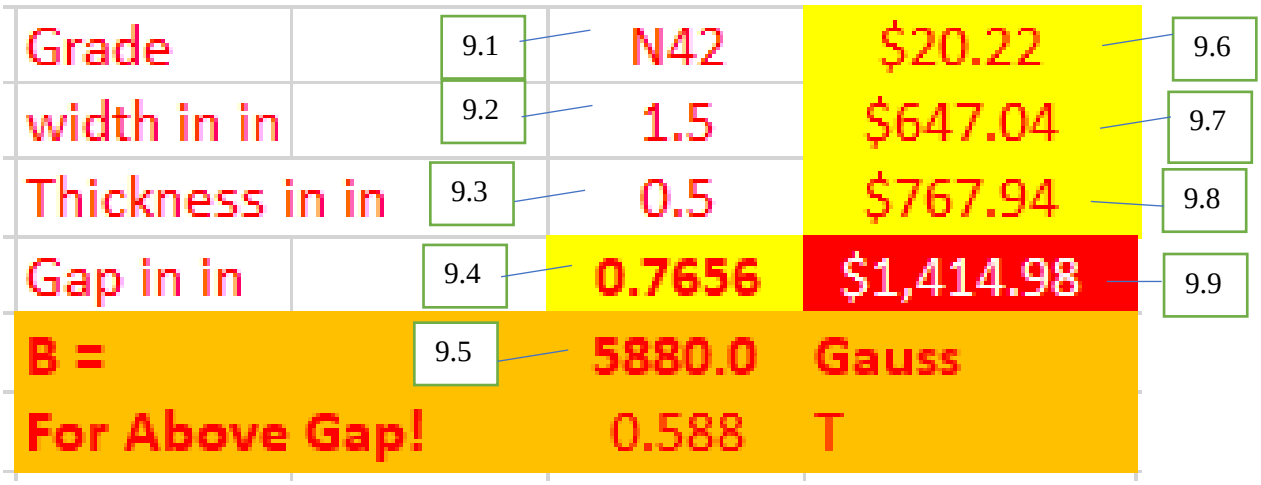

Exhibit A.9 contains the magnetic flux calculations for magnets of specified grade, geometry, and the air gap seen in Cell 5.5. As can be seen here, magnets are a very significant cost. From an economic stand point, it is ideal to try and create a model requiring the lowest grade magnet possible since each increase in grade tends to represent a significant increase in price. This price difference varies by magnet distributor.

Cell 9.1 – Magnet grade

- Even low-grade neodymium magnets are powerful. Grades may vary from 35 – 52. Magnets with grades between 40 and 52 were investigated, depending on products found online.

Cell 9.2 – Magnet width or diameter W_{mg} [in]

- This measurement is taken from the same product found online as used for the grade in Cell 9.1.

Cell 9.3 – Magnet thickness t_{mg} [in]

- This measurement is taken from the same product mentioned in Cells 9.1 and 9.2.

Cell 9.4 – Overall Air Gap AG [in]

- From Cell 5.5

Cell 9.5 – Magnetic Field Strength B [Gauss]

- This value is calculated using an online calculator by K&J Magnetics. This calculator requires input values of air gap, magnet grade, magnet thickness, and magnet diameter [18].

Cell 9.6 – Cost per magnet c_{mg}

- Value obtained from same product used for Cells 9.1-3

Cell 9.7 – Cost for all magnets $c_{mg,t}$

- Given by

$$c_{mg,t} = c_{mg} \cdot F_{mg} \cdot F_{ro}$$

- Variables F_{mg} and F_{ro} are the number of magnets per rotor and the number of rotors in the generator, respectively. Taken from exhibit A.8.

Cell 9.8 – Cost of copper wire for whole generator

- Taken from Cell 5.19

Cell 9.9 – Overall cost of magnets and wire

- Although this isn't the entire cost of the generator, the wire and magnets are by far the largest costs. The sum of the cost of the two is good starting point for budgeting for the entire generator.
- For the test model, only one stage was built and costs were only a fraction of the value shown here.

Appendix B

List of Components and Technical Drawings of Fabricated Parts

This appendix provides a list of components used for creating the single stage testing generator, as well as drawings created on SolidWorks for 8 of the 9 fabricated components. One of the fabricated components, the vertical testing stand support walls, were created during production instead of during design. The drawings in exhibits B.2 – B.9 are as they were upon completion of the computer model. The actual generator does not match these specifications in almost all cases due to the interdependency of the geometries of each part on the others. The process and justification for changes to drawings are described in Chapter 3.

B.1 List of Components

This exhibit contains a list of all components used in the fabrication of the single testing stage of the generator. It is separated into two lists: fabricated parts and incorporated parts.

Fabricated Parts:

- ¾ inch plywood stator body
- Steel test shaft
- Aluminum rotor spacer
- Two two-by-fours
- Aluminum “bookends” (x2)
- ¾ inch vertical testing stand walls (x2)
- Threaded aluminum stator support rods (x4)
- Aluminum rotor body (x2)
- Steel rotor disk (x2)

Incorporated Parts

- 12-gauge copper wire coils (x6)
- N52 1/8-inch neodymium permanent magnets (x48)
- Bearings (x2)
- 24 plastic zip-ties
- Dynamometer-to-shaft adapter

B.2 Rotor Spacer Drawing

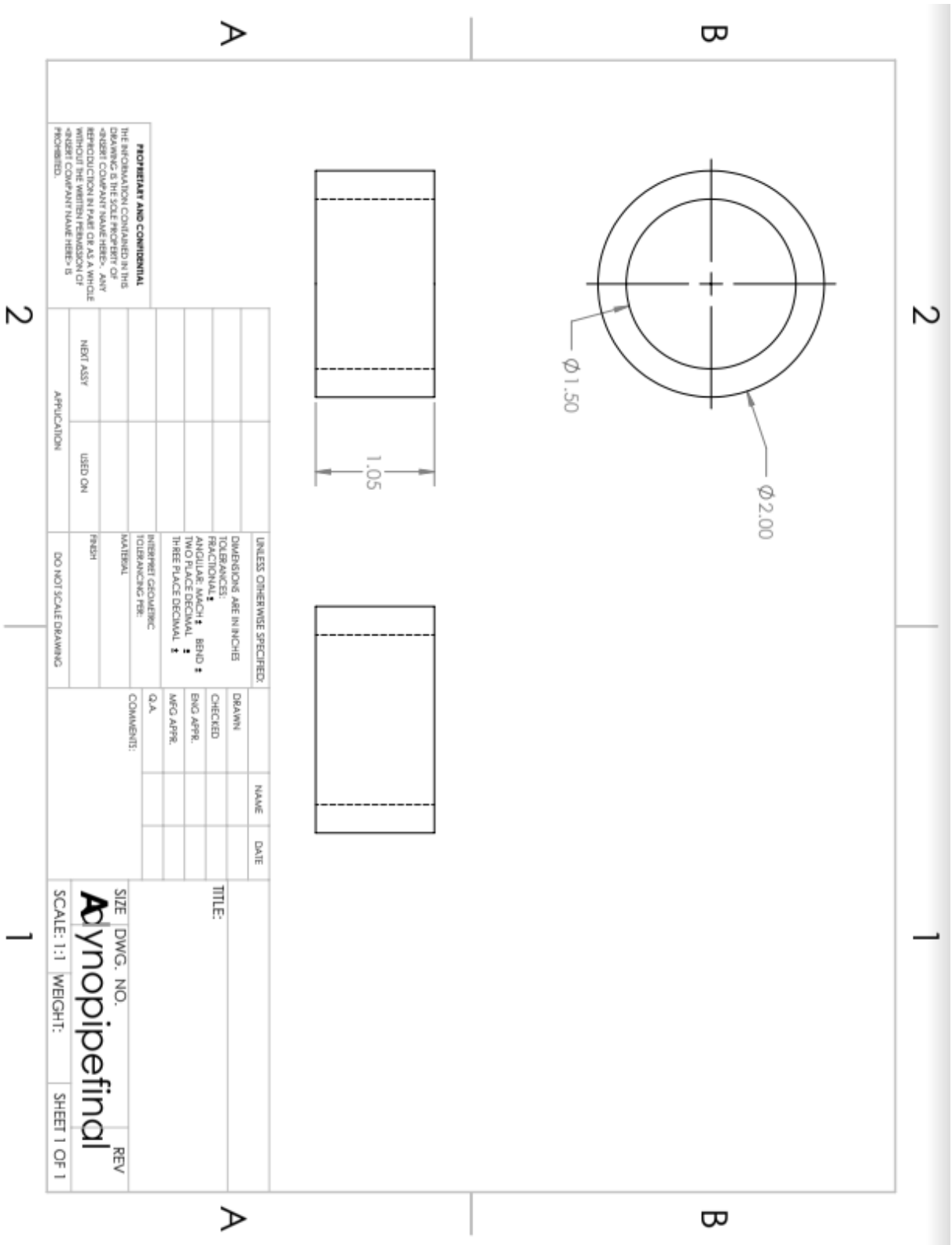

B.3 Testing Stand Base Plate

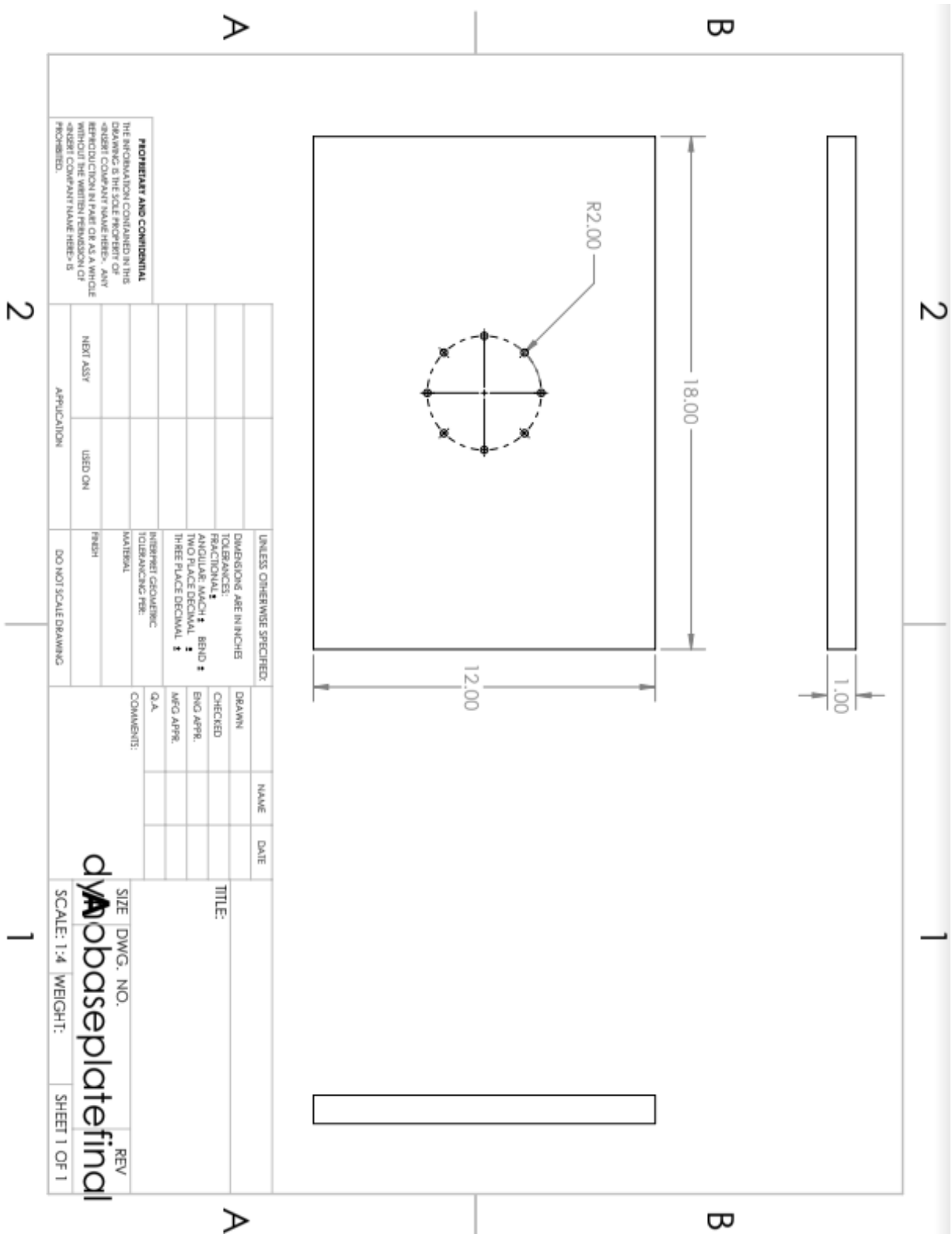

B.4 Vertical Testing Stand Wall

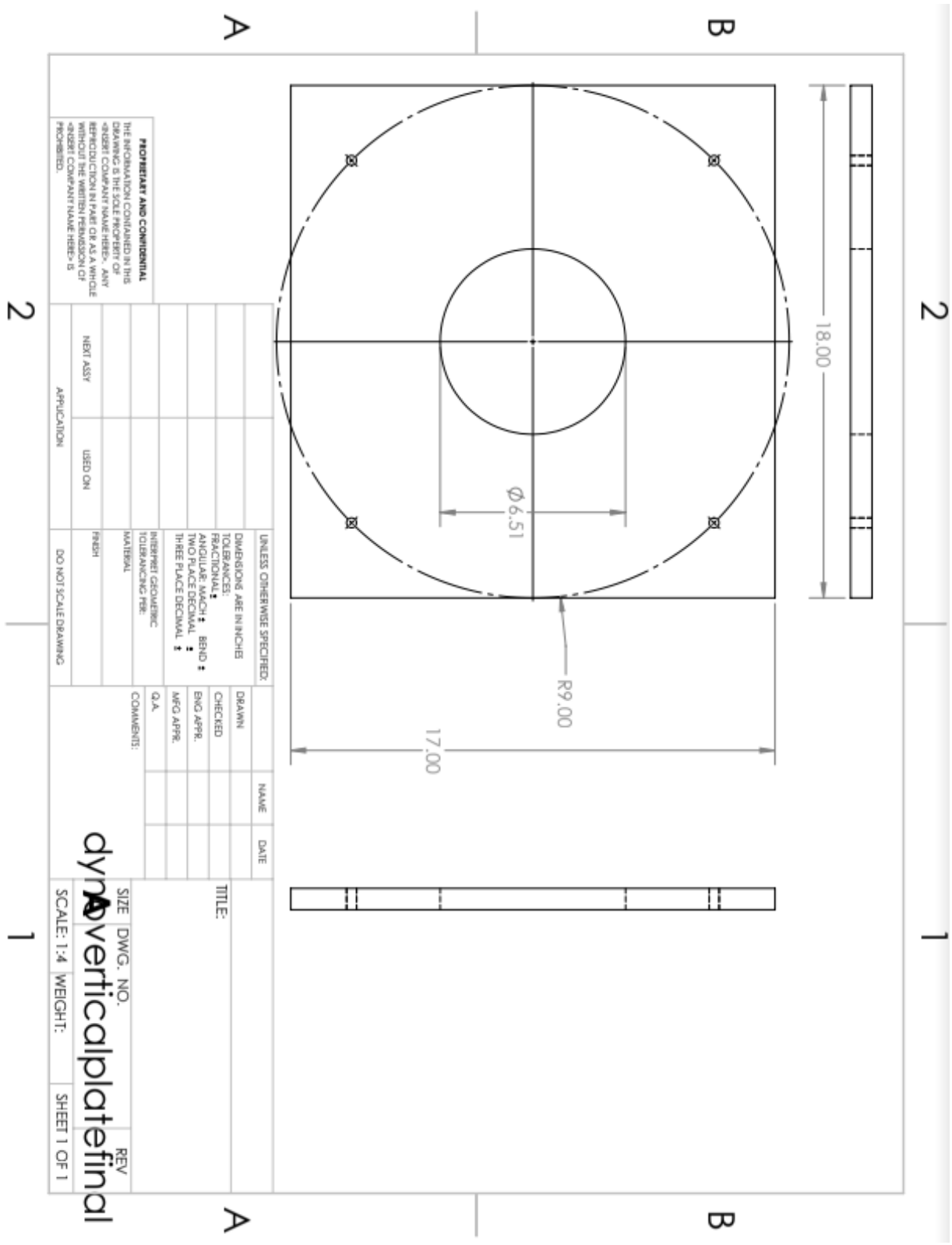

B.5 Testing Shaft

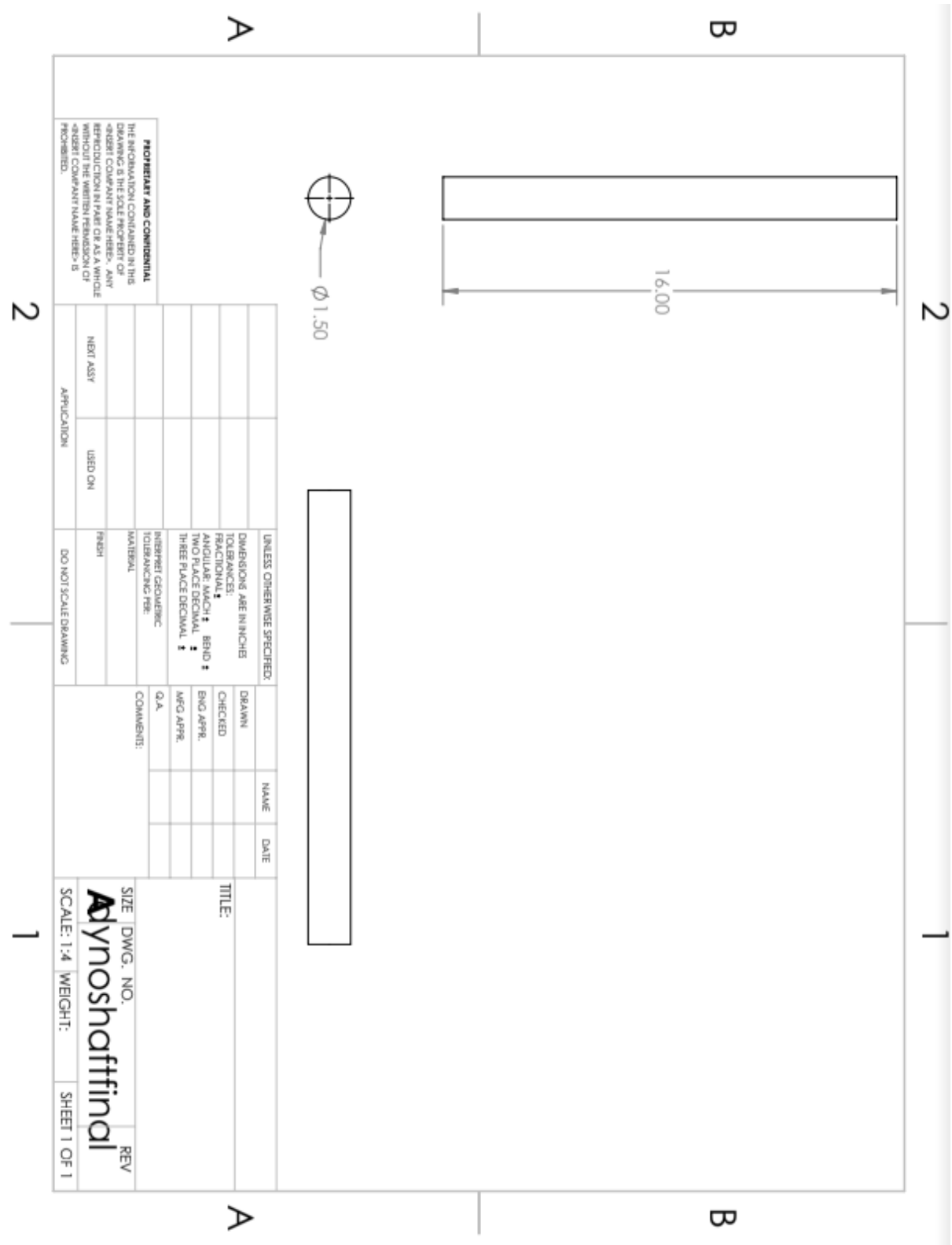

B.6 Rotor Disk

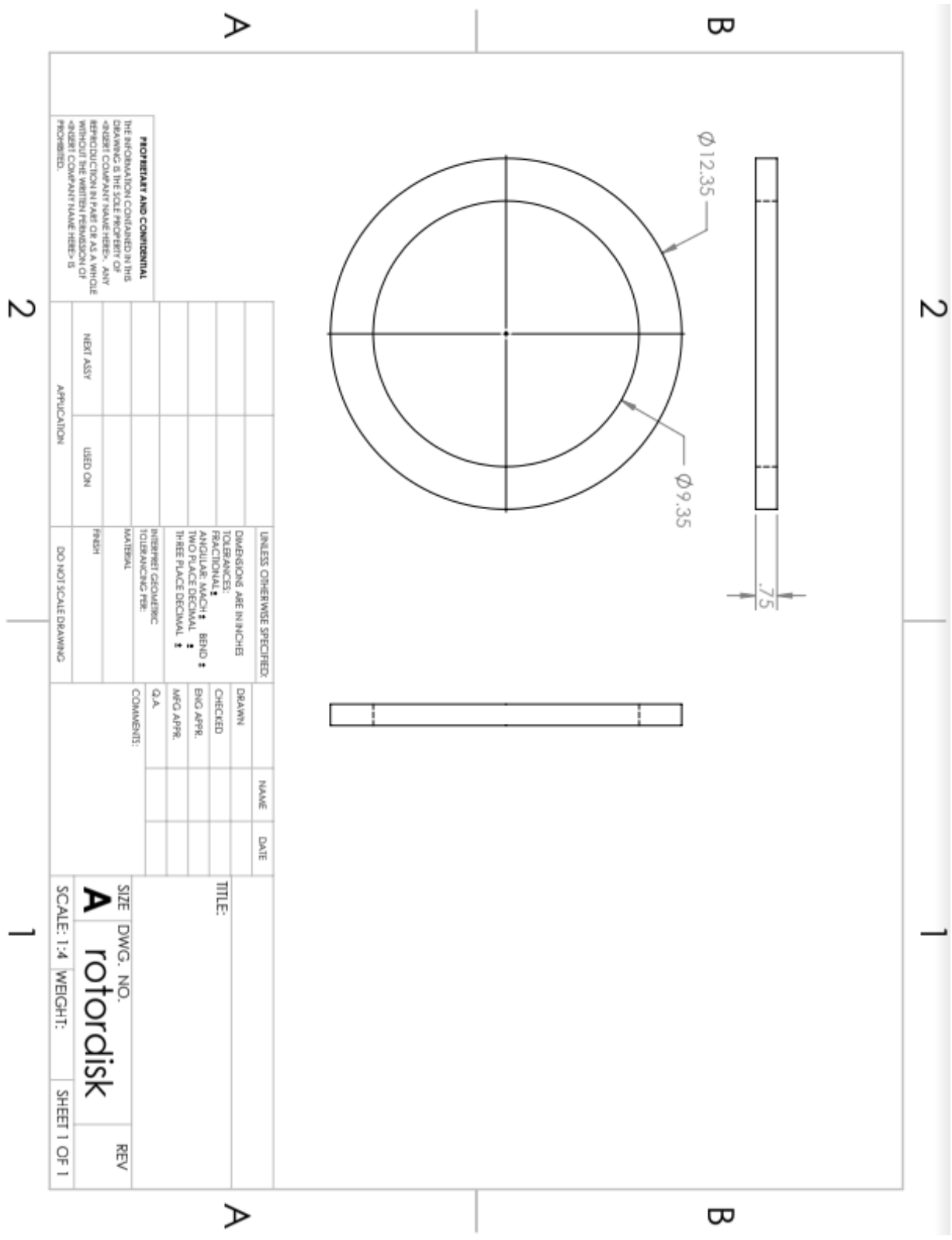

B.7 Stator Support Rod

B.8 Rotor Body

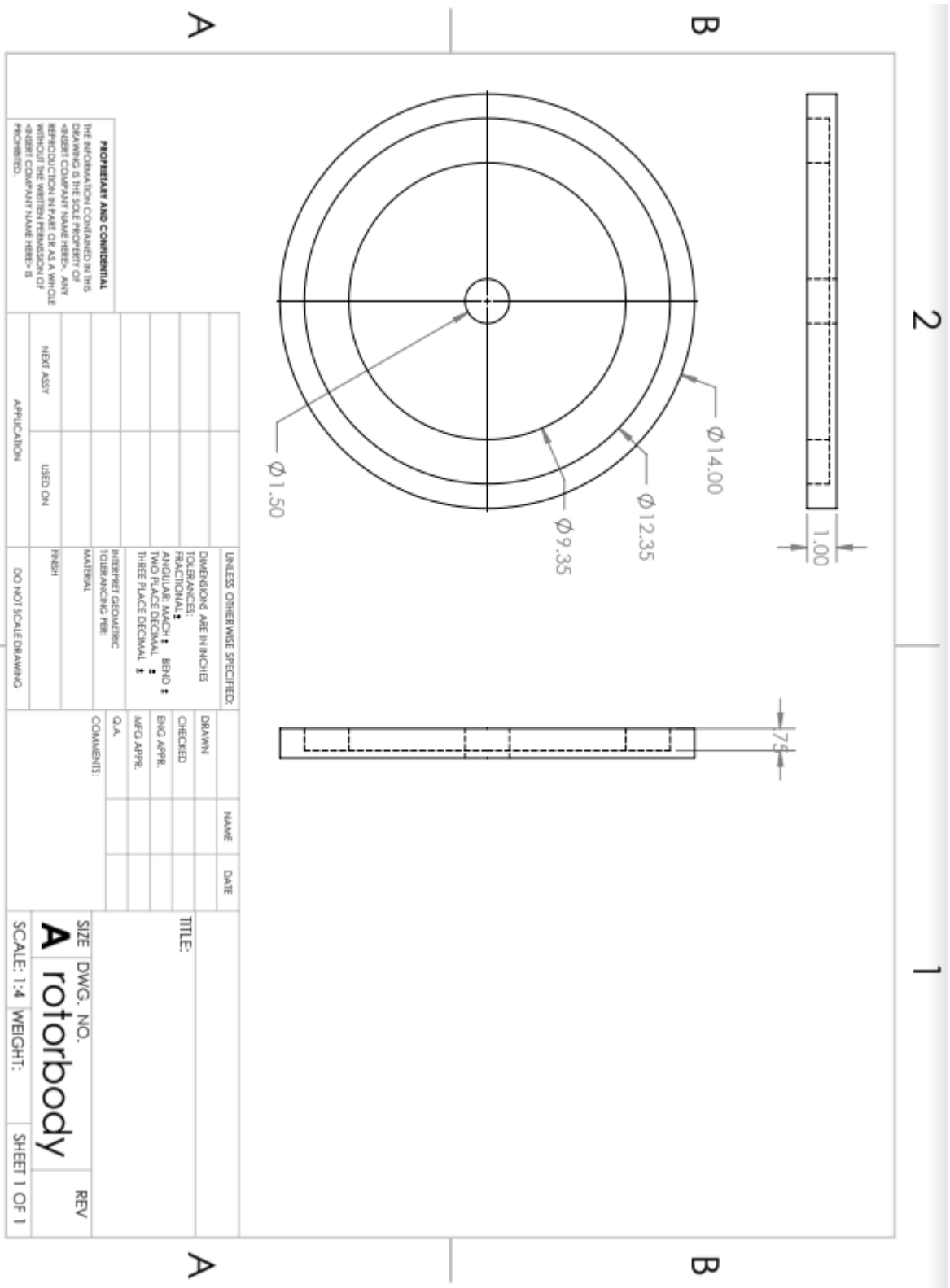

B.9 Stator Body

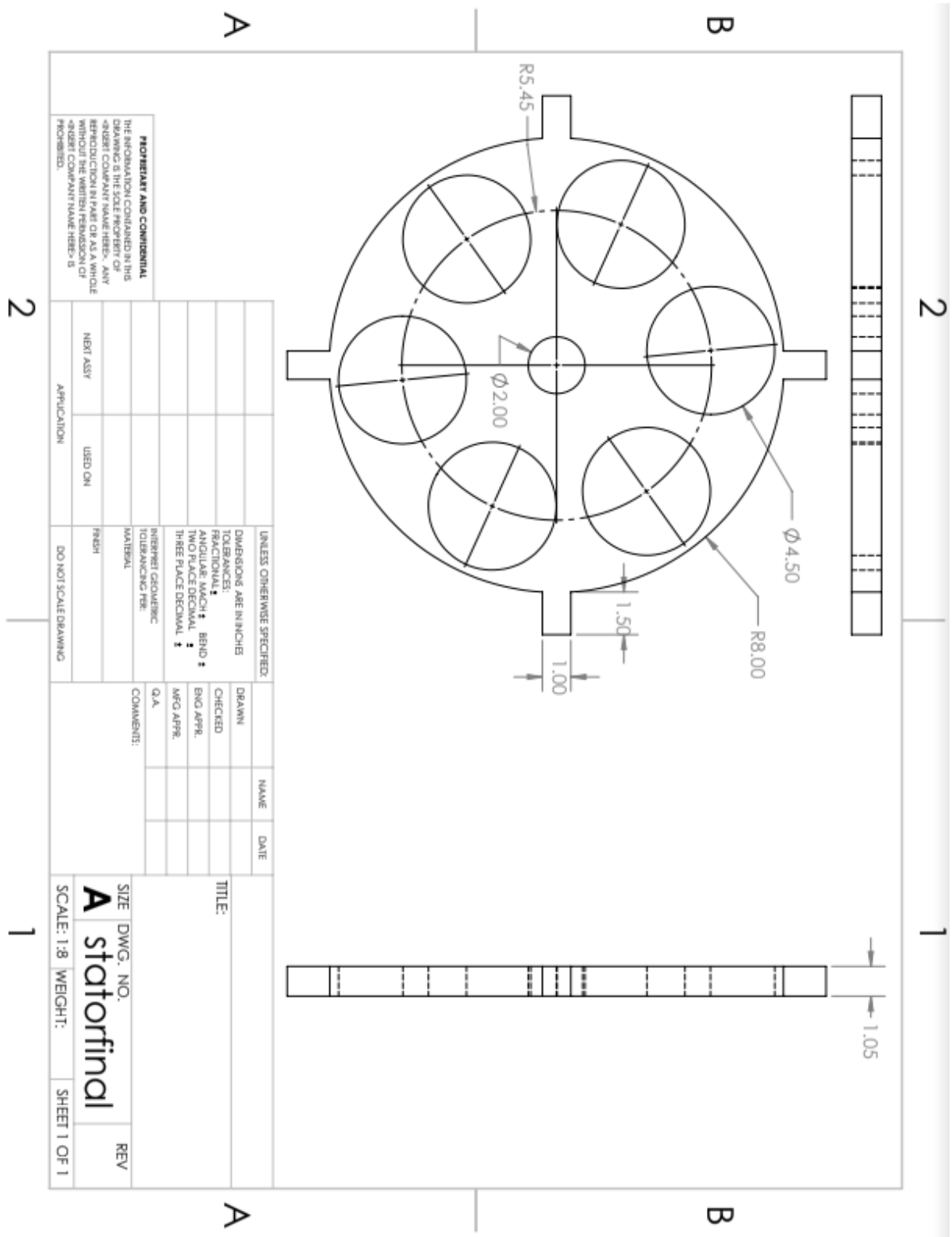

BIBLIOGRAPHY

[1] E. Moyer, "Basics of Electricity and Electrical Generation," U. Chicago, Chicago, 2010.

[2] U. A. Ghulam Ahmad, "Design, construction and study of small scale vertical axis wind turbine based on a magnetically levitated axial flux permanent magnet generator," *Renewable Energy, Vol 101,* pp. 286-292, 2015.

[3] D. J. Wagner, "Introduction to Magnetism and Induced Currents," Rensselaer Polytechnic Institute, 2001.

[4] K.C. Latoufis, G.M. Messinis, P.C. Kotsampopoulos, N.D. Hatziargyriou, "Axial Flux Permanent Magnet Generator Design for Low Cost Manufacturing of Small Wind Turbines," *Wind Engineering,* vol. 36, no. 4, pp. 411-442, 2012.

[5] M. A. Saadat Jamali Arand, "Cogging torque reduction in axial-flux permanent magnet wind generators with yokeless and segmented armature by radially segmented and peripherally shifted magnet pieces," *Renewable Energy, Vol. 99,* pp. 95-106, 2016.

[6] G.-C. Lee, S.-H. Kam and T.-U. Jung, "Design on permanent magnet structure of radial flux permanent magnet generator for cogging torque reduction and low torque ripple," in *16th European Conference on Power Electronics and Applications*, 2014.

[7] M. Joorabian and A. Zabihinejad, "Design and Construction of an optimum High Power Radial Flux Direct-drive PM Generator for Wind Applications," in *ICIEA: 2009 4th IEEE Conference on Industrial Electronics and Applications*, 2009.

[8] M. B. C. Salles, J. R. Cardoso and K. Hameyer, "Dynamic modeling of transverse flux permanent magnet generator for wind turbines," *Journal of Microwaves, Optoelectronics and Electromagnetic Applications*, vol. 10, no. 1, 2011.

[9] T. Rovio, H. Vihriala, L. Soderlund, J. Kriikka, M. Hypponen, "Axial and Radial Flux Generators in Small-Scale Wind Power Production," Tampere Unversity of Technology.

[10] Erol Kurt, Halil Gor, Umut Doner, "Electromagnetic design of a new axial and radial flux generator with the rotor back-irons," *International Journal of Hydrogen Energy, Vol 41*, pp. 7019-7026, 2015.

[11] S. Fahey, "Basic Principles of the Homemade Axial Flux Generator".

[12] C.C. Hwang, M.H. Wu, S.P. Cheng, "Influence of pole and slot combinations on cogging torque in fractional slot PM motors," *Journal of Magnetism and Magnetic Materials, Vol 304*, pp. e430-e432, 2005.

[13] M. Ç. Mehmet Recep Minaz, "Design and analysis of a new axial flux coreless PMSG with three rotors and double stators," *Results in Physics, Vol 7*, pp. 183-188, 2016.

[14] B. Wallace, "Development and Validation of a Wind Generator Field Testing Methodology," The Pennsylvania State University, 2011.

[15] B. Wallace, "Small Wind Turbine Performance Evaluation using Field Test Data and a Coupled-Aero-Electro-Mechanical Model," Pennylvania State University, 2015.

[16] Allstar Magnetics, "Neodymium Magnets," Allstar Magnetics, 2017. [Online]. Available: http://allstarmagnetics.com/neodymium_magnets/. [Accessed 18 March 2018].

[17] Thyssenkrupp Aerospace, "Materials Services," Thyssenkrupp Aerospace, 2018. [Online]. Available: http://www.thyssenkruppaerospace.com/nc/materials/steel/steel-sheet-plate/weight-calculations.html?print=1. [Accessed 18 3 2018].

[18] K&J Magnetics, "The K&J Magnetic Gap Calculator," K&J Magnetics, 2018. [Online]. Available: https://www.kjmagnetics.com/gap.calculator.asp. [Accessed July 2017].

[19] Oladapo Omotade Ogidi, Paul S. Barendse, Mohamed A. Khan, "Fault diagnosis and condition monitoring of axial-flux permanent magnet wind generators," *Electric Power Systems Research, Vol. 136,* pp. 1-7, 2015.

[20] Nihat Öztürka, Adem Dalcalıb, Emre Çelika, Selçuk Sakarc, "Cogging torque reduction by optimal design of PM synchronous generator for wind turbines," *International journal of Hydrogen Energy ,* 2016.

[21] H. Kobayashi, Y. Doi, K. Miyata, T. Minowa, "Design of the axial-flux permanent magnet coreless generator for the multi-megawatts turbine," Shin-Etsu Chemical Co, Fukui, Japan.

ACADEMIC VITA

Academic Vita of Tyler Christoffel
christoffeltyler@gmail.com

Education
Major: Mechanical Engineering
Honors: Mechanical Engineering

Thesis Title: Design, Construction, and Analysis of a Permanent Magnet Axial Flux Generator for Specific Site Conditions
Thesis Supervisor: Richard Auhl

Relevant Work Experience
Date
May 2015 – August 2015
Title
Mechanical Engineering Intern
Description
Researched mechanical failures of latest version of medical infusion pump device; proposed solutions; tested proposed solutions; created engineering reports; presented results to company executives, managing engineers.
Institution/Company (including location)
Baxter International, Medina, New York
Supervisor's Name
Troy Lindke

Grants Received: Summer Research Grant, Beier Engineering Scholarship, Schreyer Honors College Scholarship

Community Service Involvement: Alternative Fundraising Administrative Captain for Atlas Special Interest Organization 2016-2017, Alternative Fundraising Executive Chair for Atlas Special Interest Organization 2017-2018, Relay for Life Team Captain Spring 2016, Atlas general member 2014-2016